mathematics

MDPI

Article

Impact of Latent Reservoirs, Latent Infection Delays, and Treatments on HIV Dynamics

Fawaz K. Alalhareth [1,2,*], Mohammed I. Albishri [3], Mohammed H. Alharbi [3] and Miled El Hajji [3,4]

[1] Department of Mathematics, College of Arts and Sciences, Najran University, Najran, Saudi Arabia
[2] Science and Engineering Research Center, Najran University, Najran, Saudi Arabia
[3] Department of Mathematics and Statistics, Faculty of Science, University of Jeddah, P.O. Box 80327, Jeddah 21589, Saudi Arabia; malbishri0040.stu@uj.edu.sa (M.I.A.); mhhalharbi1@uj.edu.sa (M.H.A.); miled.elhajji@enit.rnu.tn (M.E.H.)
[4] ENIT-LAMSIN, Tunis El Manar University, BP. 37, Tunis-Belvédère, Tunis 1002, Tunisia
* Correspondence: fkalalhareth@nu.edu.sa

Abstract

A within-host HIV dynamics model incorporating latent reservoirs, distributed time delays, and a B-cell-mediated humoral immune response is developed and analyzed mathematically. The model includes five compartments: uninfected $CD4^+$ T cells, latently infected cells, actively infected cells, free virions, and B cells. Four distinct distributed delays are introduced to account for the periods between viral entry and the emergence of latently or actively infected cells, reactivation of latently infected cells, and intracellular virion production. For the non-delayed system, the basic reproduction number $\mathcal{R}_0$ is derived using the next-generation matrix method. Using Lyapunov functions and LaSalle's Invariance Principle, a sharp threshold dynamic is proven: the infection-free equilibrium is globally asymptotically stable (GAS) when $\mathcal{R}_0 \leq 1$, whereas a unique endemic equilibrium is GAS when $\mathcal{R}_0 > 1$. For the full distributed-delay system, a delay-dependent reproduction number $\mathcal{R}_0^d$ is defined. The global asymptotic stability of the infection-free equilibrium is established for $\mathcal{R}_0^d \leq 1$, and the global asymptotic stability of the endemic equilibrium is established for $\mathcal{R}_0^d > 1$, using suitably constructed Lyapunov functionals that account for the delay history. Numerical simulations validate the analytical threshold behavior. A sensitivity analysis of $\mathcal{R}_0^d$ identifies the most influential parameters for potential intervention. A treatment-dependent reproduction number is derived, and the critical drug efficacy required for viral eradication is determined. The intracellular production delay is shown to act as a critical threshold for infection clearance.

Keywords: HIV dynamics; latent reservoirs; infection latent delays; global stability; basic reproduction number; antiretroviral therapy

MSC: 34D23; 37N25; 92D25; 93A30

Academic Editor: Snezhana Hristova

Received: 10 April 2026
Revised: 4 May 2026
Accepted: 11 May 2026
Published: 14 May 2026

1. Introduction

Human Immunodeficiency Virus (HIV) infection remains a major global health challenge, with approximately 39 million people living with the virus and 1.3 million new infections occurring annually [1]. The within-host dynamics of HIV are extraordinarily complex, involving multiple cell types, viral replication cycles, latent reservoirs, and immune responses. Mathematical modeling has emerged as a powerful tool for unraveling this

complexity, providing insights into infection progression, treatment design, and potential eradication strategies.

A major barrier to HIV eradication is the existence of latent reservoirs, i.e., populations of resting $CD4^+$ T cells that harbor an integrated but transcriptionally silent provirus. The definitive identification of this reservoir was provided by Chun et al. [2] and Finzi et al. [3], who demonstrated that latently infected cells have an estimated half-life of approximately 44 months, making viral eradication impossible with current antiretroviral therapy (ART) alone. These cells can persist for decades and reactivate upon treatment interruption, reseeding active infection [4]. Subsequent work by Siliciano and Siliciano [5] quantified that the latent reservoir contains approximately 10^6 to 10^7 cells in infected individuals, with decay rates of only 2–3% per year under suppressive therapy.

The time lag between viral entry and the production of new virions, termed the infection latent delay, was first quantified by Herz et al. [6] using mathematical modeling of clinical data from patients treated with protease inhibitors. They estimated this intracellular delay to be approximately 1–2 days and showed that neglecting it leads to underestimation of key kinetic parameters by up to 50%. Perelson et al. [7] refined these estimates using a more detailed model of HIV-1 dynamics, demonstrating that productively infected cells have a half-life of approximately 1.6 days, while the intracellular phase contributes an additional delay of 0.9 days on average. These findings established that viral dynamics are governed not only by rates of infection and clearance but also by the timing of critical intracellular events.

The introduction of highly active antiretroviral therapy (HAART) in the mid-1990s transformed HIV from a fatal disease to a manageable chronic condition. Hammer et al. [8] showed in a landmark clinical trial that triple-drug therapy (zidovudine, lamivudine, and indinavir) reduced plasma HIV RNA to undetectable levels (<500 copies/mL) in 60–80% of patients, compared to less than 20% with dual therapy. Gulick et al. [9] demonstrated sustained viral suppression for over one year with indinavir-containing regimens, establishing the feasibility of long-term viral control. However, Paterson et al. [10] established that adherence levels below 95% are associated with a significantly increased risk of virologic failure and drug resistance, highlighting the challenges of long-term treatment. More recently, integrase strand transfer inhibitors (INSTIs) such as dolutegravir have achieved even higher efficacy, with Hightower et al. [11] reporting over 99% inhibition of viral integration.

Building on these foundational studies, mathematical modeling has become indispensable for understanding HIV pathogenesis. Herz et al. [6] and Perelson et al. [7] not only quantified viral dynamics but also established the methodological framework for estimating in vivo rate constants from clinical data. Their work revealed that the rapid turnover of HIV in blood (half-life of approximately 6 h) masks a highly dynamic process of continuous viral replication and immune-mediated killing. Since the pioneering models of [7,12], a rich literature [13–16] has developed, capturing various aspects of HIV pathogenesis through ordinary differential equations (ODEs). These models have been instrumental in quantifying viral turnover, estimating infected cell lifespans, and predicting the effects of antiretroviral therapy [17–21].

The incorporation of immune responses into HIV models has been a major focus of subsequent research. While early models focused primarily on $CD4^+$ T cell dynamics and cytotoxic T lymphocyte (CTL) responses, the role of humoral immunity mediated by B cells has received increasing attention. Murase et al. [22] were among the first to introduce B-cell dynamics into an HIV model, showing that antibody-mediated responses can reduce viral load by up to 2 logs under optimal conditions and that the timing of antibody appearance critically affects infection outcome. Their stability analysis of pathogen–immune interaction dynamics [22] demonstrated that delayed antibody responses can lead to oscillatory

behavior and that the strength of B-cell stimulation determines whether infection is cleared or becomes chronic. Subsequent work by Ganusov et al. [23] explored the role of B cells in controlling viral escape mutants, demonstrating that humoral immunity provides a crucial backup when CTL responses are compromised.

Characterizing the duration of latent infection has been approached through different mathematical frameworks. Time delay models use discrete or distributed delays to represent the intracellular phase of viral replication. Nelson and Perelson [24] developed delay differential equation models of HIV-1 infection, estimating that the average delay between infection and viral production ranges from 0.5 to 2 days, with variability depending on cell type and activation state. Culshaw and Ruan [14] analyzed a delay-differential equation model of HIV infection of $CD4^+$ T cells, showing that time delays can destabilize the system and lead to sustained oscillations.

More recently, age-structured models have provided finer resolution of infection dynamics. Rong et al. [25] used infection-age structure to show that the timing of treatment initiation critically affects the decay rate of latently infected cells, with earlier treatment leading to faster reservoir decay. Li et al. [26] extended this approach to include both CTL and antibody immune responses, demonstrating that the combination of age-structure and delayed antibody production can produce complex dynamical behaviors, including Hopf bifurcations and periodic solutions. Their analysis revealed that the delayed antibody response plays a crucial role in determining whether infection progresses to chronicity or is controlled.

The integration of latent reservoirs, time delays, and immune responses remains an active area of research. Recent studies by Prakash et al. [18] have explored bifurcation analysis in models with multiple infections and intracellular delay, while Lv et al. [19] investigated the dynamics of delayed HIV models with both viral and cellular infections. Alalhareth et al. [27] examined global dynamics and optimal control of dual-target HIV models with latent reservoirs, and Almuhashi and El Hajji [28] analyzed the effects of time delays on treatment outcomes.

While our recent works have explored various aspects of HIV dynamics [27–31], the present study introduces several distinct features that have not been previously integrated. First, whereas our previous delay models considered at most two discrete delays [28], the current model incorporates four distinct distributed delays with general probability kernels, capturing variability in (i) the time to establish latent infection, (ii) the time to establish active infection, (iii) delay in reactivation of latently infected cells, and (iv) the intracellular delay in virion production. Second, neither Ref. [27] nor Ref. [28] included any immune compartment; the current model is the first in our series to incorporate a B-cell compartment with stimulation by free virions, capturing the humoral immune response. Third, the extension to distributed delays requires fundamentally different analytical techniques: the Lyapunov functionals constructed in Section 4 incorporate memory terms that account for the entire delay history, generalizing the approach of Korobeinikov [32] beyond the discrete-delay analysis in [28]. Fourth, a novel contribution not present in any of our previous work is the derivation of an explicit expression for the critical intracellular delay τ_4^{cr} (Section 5.4), identifying pharmacological prolongation of viral maturation as a potential therapeutic strategy. Finally, our systematic sensitivity analysis of the delay parameters themselves (n_i, τ_i, F_i) reveals which biological latencies most critically affect infection outcomes, informing where therapeutic interventions might be most effective. These combined features represent a significant advance beyond our recent publications, providing the most integration of latency, distributed delays, and humoral immunity in our research program to date.

Table 1 provides a brief comparison of the previous models [27,28] with the current one.

Table 1. Comparison of the previous models [27,28] with the current one.

Feature	Current Model	[27]	[28]
Compartments	X_u, X_l, X_i, X_v, X_B	X_u, X_l, X_i, X_v	X_u, X_l, X_i, X_v
Immune response	B cells (humoral)	None	None
Delay structure	Distributed (4 delays)	None	Discrete (2 delays)
Global stability proven	Yes	Yes	Yes
Optimal control	Yes	Yes	No

The remainder of the paper is organized as follows: Section 2 formulates the model; Section 3 analyzes the ODE case; Section 4 extends the analysis to distributed delays; Section 5 presents numerical results; and Section 6 concludes with discussion and future directions.

2. Mathematical Model Derivation

In this section, we formulate a within-host mathematical model to describe the dynamics of HIV infection, incorporating biological features such as latent reservoirs, distributed time delays, and the humoral immune response mediated by B cells. The model is structured as a system of delay differential equations (DDEs) that captures the interactions between uninfected $CD4^+$ T cells, latently infected cells, actively infected cells, free virions, and B cells. Distributed delays are introduced to account for the time lags between viral entry and the emergence of infected cell populations, as well as delays in viral production and B cell activation. The model considers the stimulation of B-cell proliferation in response to viral presence, capturing the activation of the humoral immune response during HIV infection. A complete description of state variables, parameters, delay distributions, and initial conditions is provided, along with fundamental analytical results—such as the boundedness and positivity of solutions—that ensure the model's biological consistency and mathematical tractability.

The schematic diagram (Figure 1) illustrates the compartmental structure and interaction pathways of the model. It shows the five state variables—uninfected $CD4^+$ T cells (X_u), latently infected cells (X_l), actively infected cells (X_i), free virions (X_v), and B cells (X_B)—along with the infection routes (β, α), delay stages $(\omega_1, \omega_2, \omega_3, \omega_4)$, and key processes such as latent cell activation (ν), viral production (r_v), and B-cell stimulation (ε) in response to free virions.

Therefore, the proposed model illustrates the coupled, delay-dependent structure of HIV pathogenesis, emphasizing the roles of latency, delayed viral replication, and the role of B cells in antiviral response. In particular, the mathematical model provides the following key elements:

- Two routes of infection—latent ($(1-\alpha)\beta$) and active ($\alpha\beta$)—with distributed delays (ω_1, ω_2).
- Latent cells (X_l) activate at rate ν to become active cells (X_i)—with distributed delay (ω_3).
- Active cells produce virions after intracellular delay ω_4.
- The presence of HIV stimulates the proliferation of B cells at a rate $\varepsilon X_v X_B$.

For $i = 1, 2, 3, 4$, the functions $\zeta_i(\tau)$ represent probability density functions for the distributed delays, defined on $[0, \omega_i]$ with ω_i possibly infinite, satisfying

$$\zeta_i(\tau) > 0, \quad \int_0^{\omega_i} \zeta_i(\tau)\, d\tau = 1, \quad \int_0^{\omega_i} \zeta_i(\tau) e^{l\tau}\, d\tau < \infty \quad (l > 0) \text{ where } \Pi_i(\tau) = \zeta_i(\tau) e^{-n_i \tau}.$$

We define $F_i = \int_0^{\omega_i} \Pi_i(\tau)\, d\tau$, satisfying $0 < F_i \leq 1$.

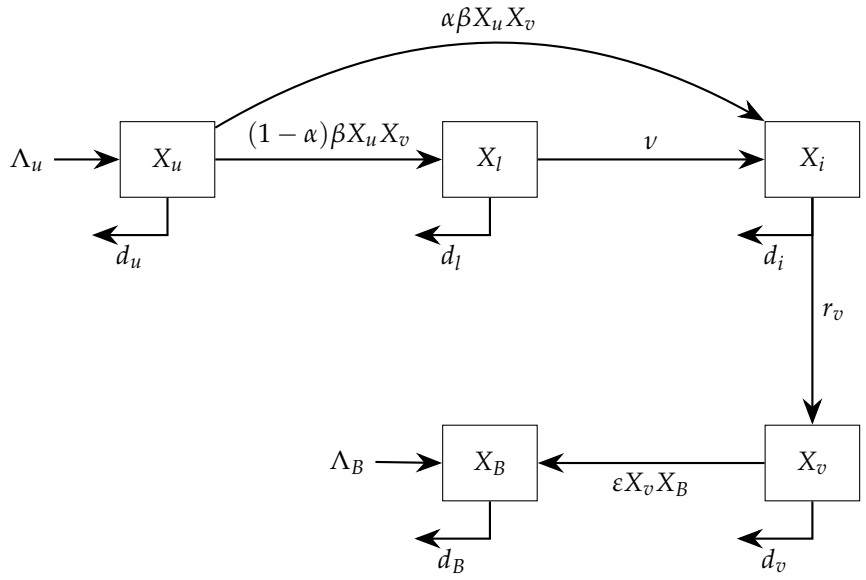

Figure 1. Schematic diagram of the HIV within-host model with latent reservoirs, distributed delays, and B cell immune response (system (1)–(5)).

Based on the schematic diagram (Figure 1), we consider the following system of delay differential equations that describes the within-host dynamics of HIV infection, taking into account latent reservoirs, distributed delays in infection and viral production, and the immune response mediated by B cells:

$$\dot{X}_u(t) = \Lambda_u - d_u X_u(t) - \beta X_u(t) X_v(t), \tag{1}$$

$$\dot{X}_l(t) = (1-\alpha)\beta \int_0^{\omega_1} \Pi_1(\tau) X_u(t-\tau) X_v(t-\tau)\, d\tau - (\nu + d_l) X_l(t), \tag{2}$$

$$\dot{X}_i(t) = \alpha\beta \int_0^{\omega_2} \Pi_2(\tau) X_u(t-\tau) X_v(t-\tau)\, d\tau + \nu \int_0^{\omega_3} \Pi_3(\tau) X_l(t-\tau)\, d\tau - d_i X_i(t), \tag{3}$$

$$\dot{X}_v(t) = r_v \int_0^{\omega_4} \Pi_4(\tau) X_i(t-\tau)\, d\tau - d_v X_v(t) - \eta X_v(t) X_B(t), \tag{4}$$

$$\dot{X}_B(t) = \Lambda_B + \varepsilon X_v(t) X_B(t) - d_B X_B(t), \tag{5}$$

for all $t > 0$.

For each delay process $i = 1, \ldots, 4$, a probability density function $\zeta_i(\tau)$ is introduced, defined on the interval $[0, \omega_i]$ with ω_i possibly infinite. These density functions satisfy $\zeta_i(\tau) > 0$ and $\int_0^{\omega_i} \zeta_i(\tau) d\tau = 1$. To incorporate both the distribution of the time lag and the decay of infected cells or virions during the delay period, the effective kernel is defined as $\Pi_i(\tau) = \zeta_i(\tau) e^{-n_i \tau}$, where $n_i \geq 0$ is a decay rate. The total contribution from all past times to a given compartment at time t is then represented by the integral $\int_0^{\omega_i} \Pi_i(\tau) Y(t-\tau) d\tau$, where Y denotes the relevant variable (e.g., $X_u X_v$ for infection terms, or X_l or X_i for activation and production terms). This formulation generalizes discrete delays (obtained when ζ_i is a Dirac delta function) and allows for more realistic distributions such as gamma or uniform delays. The net effect of each delay on the infection threshold is summarized by the factor $F_i = \int_0^{\omega_i} \Pi_i(\tau) d\tau$, which satisfies $0 < F_i \leq 1$ and appears explicitly in the delay-dependent basic reproduction number $\mathcal{R}_0^d$.

The system (1)–(5) is equipped with initial values given by continuous functions on the delay interval $[-\tau^*, 0]$:

$$X_u(\theta) = \phi_1(\theta), X_l(\theta) = \phi_2(\theta), X_i(\theta) = \phi_3(\theta), X_v(\theta) = \phi_4(\theta), X_B(\theta) = \phi_5(\theta),\ \theta \in [-\tau^*, 0], \tag{6}$$

where $\tau^* = \max\{\omega_1, \omega_2, \omega_3, \omega_4\}$, and $\phi_j \in C([-\tau^*, 0], \mathbb{R}_+)$. The equations describe the HIV dynamics on $t > 0$ with initial values given on $[-\tau^*, 0]$.

Assumption 1 (Model Assumption)**.** *The death rates satisfy:* $d_u \leq d_l \leq d_i$.

This inequality establishes a biologically motivated hierarchy for the natural turnover rates of the T-cell populations. In fact, healthy cells are the most stable, latently infected cells form a persistent reservoir, and actively infected cells are short-lived due to viral cytotoxicity and immune attack.

Biological Interpretation of Terms

- Λ_u: Constant recruitment rate of uninfected $CD4^+$ T cells.
- Λ_B: Production rate of B cells.
- β: Infection rate for both latent and active infections.
- α: Proportion of infections that directly lead to active infection. The remainder $(1 - \alpha)$ leads to latent infection.
- ν: Activation rate of latently infected cells.
- r_v: Number of virions produced per actively infected cell per unit time.
- η: Neutralization rate of virions by B cells.
- ε: Rate of B-cell proliferation stimulated by free virions. This term reflects the activation and expansion of the B-cell population in response to viral antigen, which enhances the humoral immune response.
- d_u, d_l, d_i, d_v, d_B: Death rates of uninfected T cells, latently infected cells, actively infected cells, free virions, and B cells, respectively.
- Delays account for time between infection and appearance of latently/actively infected cells (ω_1, ω_2), delay in latent cell reactivation (ω_3), and intracellular delay in virion production (ω_4).

A summary of the biological interpretation of all variables and parameters in the distributed-delay HIV model (1)–(5) is given in Table 2.

Table 2. Biological interpretation of all variables and parameters in the distributed-delay HIV model (1)–(5).

Symbol	Biological Meaning (Units Where Applicable)
$X_u(t)$	Concentration of uninfected $CD4^+$ T cells at time t (cells·mm^{-3})
$X_l(t)$	Concentration of latently infected $CD4^+$ T cells at time t (cells·mm^{-3})
$X_i(t)$	Concentration of actively infected $CD4^+$ T cells at time t (cells·mm^{-3})
$X_v(t)$	Concentration of free HIV virions in plasma/tissue at time t (virions·mm^{-3})
$X_B(t)$	Concentration of B cells (humoral immune response) at time t (cells·mm^{-3})
Λ_u	Constant recruitment rate of uninfected $CD4^+$ T cells (cells·mm^{-3}·day^{-1})
Λ_B	Constant production rate of B cells from bone marrow (cells·mm^{-3}·day^{-1})
d_u	Natural death rate of uninfected $CD4^+$ T cells (day^{-1})
d_l	Death rate of latently infected $CD4^+$ T cells (day^{-1})
d_i	Death rate of actively infected $CD4^+$ T cells (day^{-1})
d_v	Clearance rate of free virions (day^{-1})
d_B	Natural death rate of B cells (day^{-1})
β	Infection rate (mm^3·virions^{-1}·day^{-1})
α	Fraction of infections that directly lead to active infection ($0 \leq \alpha \leq 1$)
ν	Activation rate of latently infected cells into actively infected cells (day^{-1})
r_v	Viral production rate (virions·cell^{-1}·day^{-1})
η	Neutralization rate of free virions by B cells (mm^3·cells^{-1}·day^{-1})
ε	Proliferation rate of B cells stimulated by free virions (mm^3·virions^{-1}·day^{-1})

Table 2. *Cont.*

Symbol	Biological Meaning (Units Where Applicable)
ω_1	Time between infection and appearance of latently infected cells (days)
ω_2	Time between infection and appearance of actively infected cells (days)
ω_3	Delay in latent cell reactivation (days)
ω_4	Intracellular delay in virion production from actively infected cells (days)
$\zeta_i(\tau)$	Probability density function for distributed delay i, defined on $[0, \omega_i]$
$\Pi_i(\tau)$	Defined as $\Pi_i(\tau) = \zeta_i(\tau)e^{-n_i\tau}$, incorporating decay during delay
F_i	$F_i = \int_0^{\omega_i} \Pi_i(\tau)\, d\tau$, satisfies $0 < F_i \leq 1$; appears in $\mathcal{R}_0^d$
n_i	Decay rate in the delay kernel $\Pi_i(\tau)$ (day^{-1})
$\phi_j(\theta)$	Continuous initial history function for variable j on $[-\tau^*, 0]$
$\tau_{\max}$	For discrete-delay case, $\tau_{\max} = \max\{\tau_1, \tau_2, \tau_3, \tau_4\}$ (days)

Remark 1. *ω_1 and ω_2 describe the time from viral entry into a target cell until the cell becomes either latently infected (ω_1) or actively infected (ω_2). During this period, reverse transcription, integration, and transcriptional silencing (for latency) or activation (for active infection) occur. This is the establishment delay. ω_3 reflects the time from when a latently infected cell receives an activation stimulus (e.g., antigen encounter, cytokine signaling) until it transitions to an actively infected cell that produces virions. This is the reactivation delay. Thus, ω_1 and ω_3 do not double-count latency; rather, latency is the state in between. A latently infected cell exists for a period (with mean residence time $1/(\nu + d_l)$) before reactivation, and the ω_3 delay represents the intracellular signaling and transcriptional initiation steps after stimulation.*

Having established the full distributed-delay model with latent reservoirs and B-cell response, we next turn to a foundational analysis of the system in the absence of delays. This simplification allows us to derive the basic reproduction number and establish global stability properties in a more tractable setting, which will serve as a crucial benchmark for the subsequent analysis of the delayed system.

3. Global Analysis of the HIV Model Without Distributed Delays

Analyzing the non-delayed system first allows us to isolate the intrinsic dynamics of HIV infection from the effects of time lags. The threshold behavior established here provides a baseline against which the impact of distributed delays can be quantified in Section 4. This section presents an analysis of the within-host HIV dynamics model in the absence of distributed delays. By setting all delay terms to zero, system (1)–(5) reduces to a system of ordinary differential equations (ODEs) that captures the fundamental interactions between uninfected CD4$^+$ T cells, latently infected cells, actively infected cells, free virions, and B cells. The simplified model allows for a more tractable examination of the system's qualitative behavior, including the existence and stability of equilibria. We begin by establishing basic properties such as non-negativity and boundedness of solutions, ensuring the biological well-posedness of the model. Subsequently, the basic reproduction number $\mathcal{R}_0$ is derived using the next-generation matrix method, serving as a critical threshold that dictates the persistence or clearance of the infection. The global asymptotic stability of the infection-free equilibrium is proven for $\mathcal{R}_0 \leq 1$, while the existence and global stability of a unique endemic equilibrium are established for $\mathcal{R}_0 > 1$. These analytical results provide a foundational understanding of the system's long-term behavior, which will later be extended to the more complex case incorporating distributed delays.

The HIV model without distributed delays is given hereafter.

$$\dot{X}_u(t) = \Lambda_u - d_u X_u(t) - \beta X_u(t) X_v(t), \tag{7}$$
$$\dot{X}_l(t) = (1-\alpha)\beta X_u(t) X_v(t) - \nu X_l(t) - d_l X_l(t), \tag{8}$$
$$\dot{X}_i(t) = \alpha\beta X_u(t) X_v(t) + \nu X_l(t) - d_i X_i(t), \tag{9}$$
$$\dot{X}_v(t) = r_v X_i(t) - d_v X_v(t) - \eta X_v(t) X_B(t), \tag{10}$$
$$\dot{X}_B(t) = \Lambda_B + \varepsilon X_v(t) X_B(t) - d_B X_B(t), \tag{11}$$

for all $t > 0$ with initial condition $(X_u^0, X_l^0, X_i^0, X_v^0, X_B^0) \in \mathbb{R}^5_+$. The equations describe the HIV dynamics on $t > 0$ with initial values given at $t = 0$.

3.1. Basic Properties: Positivity, Boundedness, and Invariant Region

This subsection establishes the fundamental mathematical properties of the ODE system (7)–(11) that ensure its biological plausibility and analytical tractability. We first prove that all state variables, uninfected CD4$^+$ T cells $X_u(t)$, latently infected cells $X_l(t)$, actively infected cells $X_i(t)$, free virions $X_v(t)$, and B cells $X_B(t)$ remain non-negative for all time $t \geq 0$ given non-negative initial conditions. This positivity property is essential for the model to represent meaningful biological concentrations. Subsequently, we demonstrate that the solutions of the system are ultimately bounded. By constructing appropriate Lyapunov-like functions and differential inequalities, we derive explicit upper bounds for each compartment and identify a positively invariant region Γ in the non-negative orthant $\mathbb{R}^5_+$. This region acts as a global attractor, meaning all trajectories eventually enter and remain within Γ. Establishing these basic properties, positivity, boundedness, and the existence of a compact invariant set, forms the necessary foundation for the equilibrium and stability analysis carried out in the subsequent subsections. Let $d = \min\{d_u, d_i/2, d_v, d_B\}$.

Lemma 1. *Dynamics (7)–(11) admit a positively invariant attractor set given by*

$$\Gamma = \left\{ (X_u, X_l, X_i, X_v, X_B) \in \mathbb{R}^5_+ \,;\, 0 \leq X_u(t), X_l(t), X_i(t) \leq \frac{\Lambda_u}{d} + \frac{d_i \eta \Lambda_B}{2 r_v \varepsilon d}, \right.$$
$$\left. 0 \leq X_v(t) \leq \frac{2 r_v \Lambda_u}{d d_i} + \frac{\eta \Lambda_B}{\varepsilon d}, 0 \leq X_B(t) \leq \frac{2 r_v \varepsilon \Lambda_u}{d d_i \eta} + \frac{\Lambda_B}{d} \right\}.$$

Proof. We have

$$\begin{aligned}
\dot{X}_u|_{X_u=0} &= \Lambda_u > 0, \\
\dot{X}_l|_{X_l=0} &= (1-\alpha)\beta X_u X_v \geq 0, \quad \forall X_v, X_u \geq 0, \\
\dot{X}_i|_{X_i=0} &= \alpha\beta X_u X_v + \nu X_l \geq 0, \quad \forall X_v, X_u, X_l \geq 0, \\
\dot{X}_v|_{X_v=0} &= r_v X_i \geq 0, \quad \forall X_i \geq 0, \\
\dot{X}_B|_{X_B=0} &= \Lambda_B > 0.
\end{aligned}$$

Thus $(X_u, X_l, X_i, X_v, X_B)(t) \in \mathbb{R}^5_+$ for all $t \geq 0$ when $(X_u, X_l, X_i, X_v, X_B)(0) \in \mathbb{R}^5_+$. Now, let us show the boundedness of the model's solution. We we define $\psi(t)$ as

$$\psi = X_u + X_l + X_i + \frac{d_i}{2 r_v} X_v + \frac{d_i \eta}{2 r_v \varepsilon} X_B.$$

Then, we get

$$\begin{aligned}\dot{\psi} &= \dot{X}_u + \dot{X}_l + \dot{X}_i + \frac{d_i}{2r_v}\dot{X}_v + \frac{d_i\eta}{2r_v\varepsilon}\dot{X}_B \\ &= \Lambda_u - d_u X_u - \beta X_u X_v + (1-\alpha)\beta X_u X_v - \nu X_l - d_l X_l + \alpha\beta X_u X_v + \nu X_l - d_i X_i \\ &\quad + \frac{d_i}{2r_v}[r_v X_i - d_v X_v - \eta X_v X_B] + \frac{d_i\eta}{2r_v\varepsilon}[\Lambda_B + \varepsilon X_v X_B - d_B X_B] \\ &= \Lambda_u + \frac{d_i\eta\Lambda_B}{2r_v\varepsilon} - d_u X_u - d_l X_l - \frac{d_i}{2}X_i - \frac{d_i d_v}{2r_v}X_v - \frac{d_i\eta d_B}{2r_v\varepsilon}X_B \\ &\leq \Lambda_u + \frac{d_i\eta\Lambda_B}{2r_v\varepsilon} - d\left[X_u + X_l + X_i + \frac{d_i}{2r_v}X_v + \frac{d_i\eta}{2r_v\varepsilon}X_B\right] \\ &= \Lambda_u + \frac{d_i\eta\Lambda_B}{2r_v\varepsilon} - d\psi,\end{aligned}$$

Thus,

$$\psi(t) \leq \frac{\Lambda_u}{d} + \frac{d_i\eta\Lambda_B}{2r_v\varepsilon d} \quad \text{if} \quad \psi(0) \leq \frac{\Lambda_u}{d} + \frac{d_i\eta\Lambda_B}{2r_v\varepsilon d}.$$

and hence, $0 \leq \psi(t) \leq \frac{\Lambda_u}{d} + \frac{d_i\eta\Lambda_B}{2r_v\varepsilon d}$, for any $t \geq 0$.

The non-negativity of solutions implies that $0 \leq X_u(t), X_l(t), X_i(t) \leq \frac{\Lambda_u}{d} + \frac{d_i\eta\Lambda_B}{2r_v\varepsilon d}$, $0 \leq X_v(t) \leq \frac{2r_v}{d_i}\frac{\Lambda_u}{d} + \frac{\eta\Lambda_B}{\varepsilon d}$, $0 \leq X_B(t) \leq \frac{2r_v\varepsilon}{d_i\eta}\frac{\Lambda_u}{d} + \frac{\Lambda_B}{d}$ if $X_u(0) + X_l(0) + X_i(0) + \frac{d_i}{2r_v}X_v(0) + \frac{d_i\eta}{2r_v\varepsilon}X_B(0) \leq \frac{\Lambda_u}{d} + \frac{d_i\eta\Lambda_B}{2r_v\varepsilon d}$. □

3.2. Threshold Quantification and Equilibrium Analysis: The Basic Reproduction Number and Steady States

This subsection focuses on determining the long-term outcomes of the within-host HIV infection as predicted by the ODE model (7)–(11). The central object of this analysis is the basic reproduction number, denoted $\mathcal{R}_0$, which serves as a critical epidemiological threshold. $\mathcal{R}_0$ is derived using the next-generation matrix method [33,34], explicitly accounting for both direct infection pathways (via actively infected cells) and the indirect contribution from the latent reservoir. We analytically characterize all possible steady-state solutions (equilibria) of the system. The infection-free equilibrium $\mathcal{E}_0$, representing the complete clearance of the virus, is shown to always exist. Furthermore, we establish that a unique endemic (chronic) equilibrium $\mathcal{E}^*$, corresponding to a persistent infection state, exists if and only if $\mathcal{R}_0 > 1$. The proof of existence and uniqueness relies on constructing an auxiliary function and applying monotonicity arguments. This threshold condition, $\mathcal{R}_0 > 1$, precisely delineates the parameter regime where the virus can establish a sustained infection, thereby framing the subsequent stability analysis in Section 3.3. Let us start by defining the matrices $\mathbf{F}$ and $\mathbf{V}$ as follows: $\mathbf{F} = \begin{pmatrix} 0 & 0 & (1-\alpha)\beta\frac{\Lambda_u}{d_u} \\ 0 & 0 & \alpha\beta\frac{\Lambda_u}{d_u} \\ 0 & 0 & 0 \end{pmatrix}$ and $\mathbf{V} = \begin{pmatrix} \nu + d_l & 0 & 0 \\ -\nu & d_i & 0 \\ 0 & -r_v & d_v + \eta\frac{\Lambda_B}{d_B} \end{pmatrix}$. Therefore, the spectral radius representing the basic reproduction number is the dominant eigenvalue, given by

$$\mathcal{R}_0 = \rho(\mathbf{F}\mathbf{V}^{-1}) = \frac{\Lambda_u r_v \beta d_B(\nu + d_l\alpha)}{d_i d_u(d_v d_B + \eta\Lambda_B)(\nu + d_l)}.$$

Lemma 2.

- *Dynamics (7)–(11) admits a trivial steady state denoted by* $\mathcal{E}_0 = \left(\frac{\Lambda_u}{d_u}, 0, 0, 0, \frac{\Lambda_B}{d_B}\right)$.
- *If* $\mathcal{R}_0 > 1$, *then dynamics (7)–(11) admits an endemic steady state* $\mathcal{E}^* = (X_u^*, X_l^*, X_i^*, X_v^*, X_B^*)$.

Proof. Steady states are obtained by setting all equations of dynamics (7)–(11) to zero:

$$\begin{cases} 0 = \Lambda_u - d_u X_u - \beta X_u X_v, \\ 0 = (1-\alpha)\beta X_u X_v - \nu X_l - d_l X_l, \\ 0 = \alpha\beta X_u X_v + \nu X_l - d_i X_i, \\ 0 = r_v X_i - d_v X_v - \eta X_v X_B, \\ 0 = \Lambda_B + \varepsilon X_v X_B - d_B X_B. \end{cases}$$

We find that the given model (7)–(11) has two equilibria:

- Infection-free equilibrium, $\mathcal{E}_0 = \left(\frac{\Lambda_u}{d_u}, 0, 0, 0, \frac{\Lambda_B}{d_B}\right)$.
- Endemic equilibrium, $\mathcal{E}^* = (X_u^*, X_l^*, X_i^*, X_v^*, X_B^*)$, where

$$X_u^* = \frac{(\nu + d_l)X_l^*}{(1-\alpha)\beta X_v^*}, X_l^* = \frac{d_i(1-\alpha)X_i^*}{(\nu + d_l\alpha)}, X_i^* = \frac{d_v X_v^* + \eta X_v^* X_B^*}{r_v}, X_B^* = \frac{\Lambda_B}{d_B - \varepsilon X_v^*},$$

where $0 < X_v^* < \frac{d_B}{\varepsilon}$, which satisfies the following equation: $a_1 X_v^2 + a_2 X_v + a_3 = 0$, where

$$\begin{aligned} a_1 &= d_i d_v \beta\varepsilon(\nu + d_l), \\ a_2 &= d_i d_u d_v \varepsilon(\nu + d_l) - d_i d_v \beta d_B(\nu + d_l) - d_i \eta\Lambda_B\beta(\nu + d_l) - \Lambda_u r_v \beta\varepsilon(\nu + d_l\alpha), \\ a_3 &= \Lambda_u r_v \beta d_B(\nu + d_l\alpha) - d_i d_u d_v d_B(\nu + d_l) - d_i d_u \eta\Lambda_B(\nu + d_l). \end{aligned}$$

We define the quadratic function $\Phi(X_v)$ as $\Phi(X_v) = a_1 X_v^2 + a_2 X_v + a_3$. Since $a_1 = d_i d_v \beta\varepsilon(\nu + d_l) > 0$, Φ is a strictly convex function on $\mathbb{R}$. Furthermore, we have

$$\begin{aligned} \Phi(0) &= \Lambda_u r_v \beta d_B(\nu + d_l\alpha) - d_i d_u d_v d_B(\nu + d_l) - d_i d_u \eta\Lambda_B(\nu + d_l) \\ &= d_i d_u(\nu + d_l)(\eta\Lambda_B + d_v d_B)(\mathcal{R}_0 - 1). \end{aligned}$$

Therefore, $\Phi(0) > 0$ if $\mathcal{R}_0 > 1$ as well as $\Phi\left(\frac{d_B}{\varepsilon}\right) < 0$. Since Φ is continuous on $\left[0, \frac{d_B}{\varepsilon}\right]$, the intermediate value theorem ensures the existence of at least one $X_v^* \in \left(0, \frac{d_B}{\varepsilon}\right)$ such that $\Phi(X_v^*) = 0$. Since $a_1 > 0$, the function Φ is strictly convex, and therefore, it can have at most two real roots. Moreover, its derivative is $\Phi'(X) = 2a_1 X + a_2$, which is strictly increasing on $\mathbb{R}$.
Assume, for contradiction, that Φ admits two distinct positive roots $0 < X_1 < X_2$. Then, by Rolle's theorem, there exists $c \in (X_1, X_2)$ such that

$$\Phi'(c) = 0.$$

Since Φ' is strictly increasing, it has exactly one zero, given by $X_{\min} = -\frac{a_2}{2a_1}$. Thus, Φ decreases on $(-\infty, X_{\min})$ and increases on $(X_{\min}, +\infty)$.

Now, since $\Phi(0) > 0$ and $\Phi\left(\frac{d_B}{\varepsilon}\right) < 0$, the function must be strictly decreasing at least on an interval starting from 0, which implies $X_{\min} > 0$. Therefore, Φ is strictly decreasing on $(0, X_{\min})$ and strictly increasing on $(X_{\min}, +\infty)$.

This implies that Φ can cross the horizontal axis at most once in $(0, X_{\min})$ and at most once in $(X_{\min}, +\infty)$. However, since $\Phi(0) > 0$ and $\Phi\left(\frac{d_B}{\varepsilon}\right) < 0$, the sign change occurs before reaching the minimum point $X_{\min}$. Hence, the root lies in the strictly decreasing region $(0, X_{\min})$. Consequently, Φ can admit only one root in the interval $\left(0, \frac{d_B}{\varepsilon}\right)$.

Thus, there exists a unique X_v^* such that $0 < X_v^* < \frac{d_B}{\varepsilon}$ satisfies $\Phi(X_v^*) = 0$. As a result, we get $X_u^* > 0$, $X_l^* > 0$, $X_i^* > 0$ and $X_B^* > 0$.

□

3.3. Global Stability Analysis of Equilibria

This subsection establishes the global asymptotic stability properties of the equilibria identified in Section 3.2, providing a complete qualitative picture of the system's long-term dynamics for all possible initial conditions. We employ the method of Lyapunov functions, constructing suitable scalar energy-like functions for each equilibrium [35]. First, for the case $\mathcal{R}_0 \leq 1$, we prove that the infection-free equilibrium $\mathcal{E}_0$ is globally asymptotically stable (GAS). This result implies that regardless of the initial viral load, the infection will be cleared from the host if the basic reproduction number is at or below unity. Conversely, when $\mathcal{R}_0 > 1$, we demonstrate that the unique endemic equilibrium $\mathcal{E}^*$ is GAS. This means the system will converge to the chronic infection state for any non-trivial initial condition, confirming the epidemiological threshold established earlier. The proofs leverage the classical LaSalle's Invariance Principle and careful algebraic manipulations to show the negativity of the Lyapunov derivatives. These global stability results confirm the threshold dynamics governed solely by $\mathcal{R}_0$, with no possibility of bistability or oscillatory persistence in the non-delayed model.

Define H as the nonnegative function $H(z) = z - 1 - \ln z$ that only vanishes at $z = 1$.

Theorem 1. *The trivial equilibrium point $\mathcal{E}_0$ is globally asymptotically stable once $\mathcal{R}_0 \leq 1$.*

Proof. The proof is based on the Lyapunov function $\mathcal{F}_0(X_u, X_l, X_i, X_v, X_B)$ given by

$$\mathcal{F}_0 = \frac{\Lambda_u}{d_u} H\left(\frac{d_u X_u}{\Lambda_u}\right) + \frac{\nu}{\nu + d_l\alpha} X_l + \frac{\nu + d_l}{\nu + d_l\alpha} X_i + \frac{d_i(\nu + d_l)}{r_v(\nu + d_l\alpha)} X_v + \frac{d_i\eta(\nu + d_l)}{r_v\varepsilon(\nu + d_l\alpha)} \frac{\Lambda_B}{d_B} H\left(\frac{d_B X_B}{\Lambda_B}\right).$$

and uses LaSalle's Invariance Principle [36] to prove that $\mathcal{E}_0$ is GAS if $\mathcal{R}_0 \leq 1$. More details are given in Appendix A.1. □

Theorem 2. *The endemic equilibrium $\mathcal{E}^*$ is GAS when $\mathcal{R}_0 > 1$.*

Proof. The proof is based on the Lyapunov function $\mathcal{F}^*(X_u, X_l, X_i, X_v, X_B)$ given by

$$\begin{aligned}\mathcal{F}^* = \; & X_u^* H\left(\frac{X_u}{X_u^*}\right) + \frac{\nu}{(\nu + d_l\alpha)} X_l^* H\left(\frac{X_l}{X_l^*}\right) + \frac{(\nu + d_l)}{(\nu + d_l\alpha)} X_i^* H\left(\frac{X_i}{X_i^*}\right) \\ & + \frac{d_i(\nu + d_l)}{r_v(\nu + d_l\alpha)} X_v^* H\left(\frac{X_v}{X_v^*}\right) + \frac{d_i\eta(\nu + d_l)}{r_v\varepsilon(\nu + d_l\alpha)} X_B^* H\left(\frac{X_B}{X_B^*}\right).\end{aligned}$$

and by using LaSalle's Invariance Principle [36] to prove that $\mathcal{E}^*$ is GAS if $\mathcal{R}_0 > 1$. More details are given in Appendix A.2. □

In conclusion, Section 3 has provided a complete analytical framework for the within-host HIV model in the absence of distributed delays. We established the model's well-posedness by proving the positivity and ultimate boundedness of solutions, confining the dynamics to a biologically relevant invariant region Γ. The critical threshold for infection persistence was precisely quantified through the basic reproduction number $\mathcal{R}_0$, derived via the next-generation matrix method. Our analysis demonstrated that the system exhibits a sharp threshold dynamic: when $\mathcal{R}_0 \leq 1$, the infection-free equilibrium $\mathcal{E}_0$ is globally asymptotically stable, guaranteeing viral clearance, whereas when $\mathcal{R}_0 > 1$, a unique endemic equilibrium $\mathcal{E}^*$ emerges and is globally asymptotically stable, leading to chronic infection. These results, proven using Lyapunov function techniques and LaSalle's Invariance Principle, establish a solid foundation for understanding the basic interaction dynamics. The insights gained here form a crucial benchmark against which the more complex effects of distributed delays, analyzed in the subsequent section, can be evaluated.

4. Dynamics with Distributed Delays: Incorporating Realistic Time Lags

This section extends the analysis of the within-host HIV model by incorporating distributed time delays, which account for essential biological latencies in the infection process. The model (1)–(5) generalizes the ODE system (7)–(11) by introducing four distinct distributed delays: ω_1 and ω_2 for the time between viral entry and the emergence of latently and actively infected cells, respectively; ω_3 for the intracellular delay in virion production; and ω_4 for the delay in B-cell activation. These delays are modeled using general probability density functions $\zeta_i(\tau)$, making the framework adaptable to various delay distributions (e.g., discrete, gamma-distributed). We begin by establishing the fundamental properties of the delay system, including the non-negativity and ultimate boundedness of solutions, and identify a positively invariant attracting region. Subsequently, we derive the corresponding basic reproduction number $\mathcal{R}_0^d$, which incorporates the delay kernels through integral factors F_i. We prove the existence of a unique endemic equilibrium when $\mathcal{R}_0^d > 1$. The core of this section is dedicated to proving the global asymptotic stability of both the infection-free equilibrium (for $\mathcal{R}_0^d \leq 1$) and the endemic equilibrium (for $\mathcal{R}_0^d > 1$), employing suitably constructed Lyapunov functionals that explicitly account for the distributed delays. This analysis reveals how time lags quantitatively alter the threshold condition and system dynamics while preserving the qualitative threshold behavior established in the non-delayed case.

4.1. Basic Properties of the Delay System

This subsection establishes the fundamental mathematical properties of the distributed-delay HIV model given by system (1)–(5). Ensuring the biological plausibility and analytical tractability of the model requires proving that its solutions remain nonnegative at all times—reflecting the physical reality of cell and virus concentrations—and that they are ultimately bounded within a biologically feasible region. We demonstrate the nonnegativity of solutions using a recursive argument based on the form of the equations and the nonnegative initial conditions specified in (6). Subsequently, we prove the ultimate boundedness of all state variables by constructing appropriate auxiliary functions and deriving differential inequalities that yield explicit upper bounds. These bounds collectively define a compact, positively invariant set Γ in the nonnegative orthant $\mathbb{R}^5_+$, which acts as a global attractor for the system's trajectories. Establishing these basic properties—nonnegativity, boundedness, and the existence of an invariant region—forms the essential foundation for all subsequent equilibrium and stability analysis in the presence of distributed delays, guaranteeing that the model is well-posed and that its long-term dynamics are confined to a biologically meaningful domain.

Lemma 3. *Solutions of model (1)–(5) with the initial states (6) are nonnegative and ultimately bounded. Furthermore, the set*

$$\Gamma = \Big\{ (X_u, X_l, X_i, X_v, X_B) \in C_+^5 : \|X_u\| \le \frac{\Lambda_u}{d_u}, \|X_l\| \le \frac{(1-\alpha)\Lambda_u}{d_u}, \|X_i\| \le \frac{\alpha\Lambda_u}{d_u} + \frac{\nu(1-\alpha)\Lambda_u}{d_u^2},$$
$$\|X_v\| \le \frac{r_v\alpha\Lambda_u}{\zeta d_u} + \frac{\nu r_v(1-\alpha)\Lambda_u}{\zeta d_u^2} + \frac{\eta\Lambda_B}{\varepsilon\zeta}, \|X_B\| \le \frac{\varepsilon r_v\alpha\Lambda_u}{\eta\zeta d_u} + \frac{\varepsilon r_v\nu(1-\alpha)\Lambda_u}{\eta\zeta d_u^2} + \frac{\Lambda_B}{\zeta} \Big\}$$

is positively invariant with respect to model (1)–(5).

Proof. Let us show the nonnegativity of solutions of model (1)–(5). Clearly, Equations (1) and (5) of model (1)–(5) give

$$\dot{X}_u\big|_{X_u=0} = \Lambda_u > 0, \quad \dot{X}_B\big|_{X_B=0} = \Lambda_B > 0.$$

Hence, $X_u(t) > 0$ and $X_B(t) > 0$ for any $t \ge 0$. In addition, we have

$$\begin{aligned}
X_l(t) &= \phi_2(0)e^{-(\nu+d_l)t} + (1-\alpha)\beta\int_0^t e^{-(\nu+d_l)(t-\theta)}\int_0^{\omega_1}\Pi_1(\tau)X_u(\theta-\tau)X_v(\theta-\tau)\,d\tau d\theta \ge 0,\\
X_i(t) &= \phi_3(0)e^{-d_i t} + \int_0^t e^{-d_i(t-\theta)}\Big[\alpha\beta\int_0^{\omega_2}\Pi_2(\tau)X_u(\theta-\tau)X_v(\theta-\tau)\,d\tau\\
&\qquad + \nu\int_0^{\omega_3}\Pi_3(\tau)X_l(\theta-\tau)\,d\tau\Big]d\theta \ge 0,\\
X_v(t) &= \phi_4(0)e^{-\int_0^t(d_v+\eta X_B(x))dx}\\
&\qquad + r_v\int_0^t e^{-\int_\theta^t(d_v+\eta X_B(x))dx}\int_0^{\omega_4}\Pi_4(\tau)X_i(\theta-\tau)\,d\tau d\theta \ge 0,
\end{aligned}$$

for any $t \in [0, \tau^*]$. Hence, by recursive argumentation, we obtain $(X_l, X_i, X_v)(t) \ge 0$ for any $t \ge 0$.

Let us prove the ultimate boundedness of solution $(X_u, X_l, X_i, X_v, X_B)$. From Equation (1), we have $\limsup_{t\to\infty} X_u(t) \le \frac{\Lambda_u}{d_u}$. To prove the ultimate boundedness of $X_l(t)$, we define

$$\psi_1 = (1-\alpha)\int_0^{\omega_1}\Pi_1(\tau)X_u(t-\tau)\,d\tau + X_l.$$

Then, we get

$$\begin{aligned}
\dot{\psi}_1 &= (1-\alpha)\Lambda_u\int_0^{\omega_1}\Pi_1(\tau)\,d\tau - (1-\alpha)d_u\int_0^{\omega_1}\Pi_1(\tau)X_u(t-\tau)\,d\tau - (\nu+d_l)X_l\\
&\le (1-\alpha)\Lambda_u F_1 - d_u\Big[(1-\alpha)\int_0^{\omega_1}\Pi_1(\tau)X_u(t-\tau)\,d\tau + X_l\Big]\\
&\le (1-\alpha)\Lambda_u - d_u\psi_1.
\end{aligned}$$

It follows that

$$\limsup_{t\to\infty}\psi_1(t) \le \frac{(1-\alpha)\Lambda_u}{d_u},$$

and then

$$\limsup_{t\to\infty} X_l(t) \le \frac{(1-\alpha)\Lambda_u}{d_u}.$$

Define

$$\psi_2 = \alpha\int_0^{\omega_2}\Pi_2(\tau)X_u(t-\tau)\,d\tau + X_i.$$

Then, we get

$$\begin{aligned}\dot{\psi}_2 &= \alpha\Lambda_u \int_0^{\omega_2} \Pi_2(\tau)\, d\tau - d_u\alpha \int_0^{\omega_2} \Pi_2(\tau) X_u(t-\tau)\, d\tau + \nu \int_0^{\omega_3} \Pi_3(\tau) X_l(t-\tau)\, d\tau - d_i X_i \\ &\leq \alpha\Lambda_u F_2 + \nu F_3 \frac{(1-\alpha)\Lambda_u}{d_u} - d_u \left[\alpha \int_0^{\omega_2} \Pi_2(\tau) X_u(t-\tau)\, d\tau + X_i\right] \\ &\leq \alpha\Lambda_u + \nu \frac{(1-\alpha)\Lambda_u}{d_u} - d_u\psi_2.\end{aligned}$$

It follows that

$$\limsup_{t\to\infty} \psi_2(t) \leq \frac{\alpha\Lambda_u}{d_u} + \nu\frac{(1-\alpha)\Lambda_u}{d_u^2},$$

then

$$\limsup_{t\to\infty} X_i(t) \leq \frac{\alpha\Lambda_u}{d_u} + \nu\frac{(1-\alpha)\Lambda_u}{d_u^2}.$$

Now, let us define

$$\psi_3 = X_v + \frac{\eta}{\varepsilon} X_B.$$

Then, we obtain

$$\begin{aligned}\dot{\psi}_3 &= r_v \int_0^{\omega_4} \Pi_4(\tau) X_i(t-\tau)\, d\tau - d_v X_v - \eta X_v X_B + \frac{\eta}{\varepsilon}(\Lambda_B + \varepsilon X_v X_B - d_B X_B) \\ &= r_v \int_0^{\omega_4} \Pi_4(\tau) X_i(t-\tau)\, d\tau - d_v X_v + \frac{\eta\Lambda_B}{\varepsilon} - \frac{\eta d_B}{\varepsilon} X_B \\ &\leq r_v \int_0^{\omega_4} \Pi_4(\tau) X_i(t-\tau)\, d\tau + \frac{\eta\Lambda_B}{\varepsilon} - d_v X_v - \frac{\eta d_B}{\varepsilon} X_B \\ &\leq r_v F_4\left(\frac{\alpha\Lambda_u}{d_u} + \nu\frac{(1-\alpha)\Lambda_u}{d_u^2}\right) + \frac{\eta\Lambda_B}{\varepsilon} - \zeta\left[X_v + \frac{\eta}{\varepsilon} X_B\right] \\ &\leq \frac{r_v\alpha\Lambda_u}{d_u} + \frac{r_v\nu(1-\alpha)\Lambda_u}{d_u^2} + \frac{\eta\Lambda_B}{\varepsilon} - \zeta\psi_3,\end{aligned}$$

where $\zeta = \min\{d_v, d_B\}$. It follows that

$$\limsup_{t\to\infty} \psi_3(t) \leq \frac{r_v}{\zeta}\frac{\alpha\Lambda_u}{d_u} + \nu\frac{r_v}{\zeta}\frac{(1-\alpha)\Lambda_u}{d_u^2} + \frac{\eta\Lambda_B}{\varepsilon\zeta},$$

and thus,

$$\limsup_{t\to\infty} X_v(t) \leq \frac{r_v}{\zeta}\frac{\alpha\Lambda_u}{d_u} + \nu\frac{r_v}{\zeta}\frac{(1-\alpha)\Lambda_u}{d_u^2} + \frac{\eta\Lambda_B}{\varepsilon\zeta}$$

and

$$\limsup_{t\to\infty} X_B(t) \leq \frac{\varepsilon}{\eta}\frac{r_v}{\zeta}\frac{\alpha\Lambda_u}{d_u} + \nu\frac{\varepsilon}{\eta}\frac{r_v}{\zeta}\frac{(1-\alpha)\Lambda_u}{d_u^2} + \frac{\Lambda_B}{\zeta}.$$

□

4.2. Equilibria and Thresholds

This subsection establishes the existence and uniqueness of equilibrium points for the distributed-delay HIV model (1)–(5) and derives the corresponding basic reproduction number $\mathcal{R}_0^d$. The analysis proceeds by setting the time derivatives in system (1)–(5) to zero and solving the resulting algebraic equations. Two distinct steady states are identified: the infection-free equilibrium $\mathcal{E}_0^d$, which always exists and represents the complete absence of the virus, and an endemic equilibrium $\mathcal{E}_*^d$, which exists if and only if the basic reproduction number exceeds unity. The threshold $\mathcal{R}_0^d$ is derived via the next-generation matrix method [34] applied to the linearized system at the infection-free state. Crucially, $\mathcal{R}_0^d$ incor-

porates the distributed-delay kernels through the integral factors $F_i = \int_0^{\omega_i} \zeta_i(\tau) e^{-n_i \tau} d\tau$, which quantify the net effect of the time lags on viral transmission and progression. This generalized reproduction number reduces to the non-delay counterpart $\mathcal{R}_0$ when all delays vanish ($F_i = 1$). The existence proof for the endemic equilibrium employs an auxiliary function and monotonicity arguments, demonstrating a unique biologically feasible chronic-infection state when $\mathcal{R}_0^d > 1$. These results extend the threshold analysis of Section 3 to the more realistic setting with distributed delays, confirming that the qualitative threshold dynamics—characterized by a transcritical bifurcation at $\mathcal{R}_0^d = 1$—are preserved despite the incorporation of biological latencies [37].

We proceed by calculating the delayed reproduction number R_0^d by deriving it from the linearization of the distributed-delay system around the disease-free equilibrium (DFE), and by showing how the delay kernels lead naturally to the appearance of the factors F_i [34,38].

From the model (1)–(5), the disease-free equilibrium is

$$E_0^d = \left(\frac{\Lambda_u}{d_u}, 0, 0, 0, \frac{\Lambda_B}{d_B} \right).$$

Let us define the infected variables vector

$$\mathbf{x}(t) = \begin{pmatrix} X_l(t) \\ X_i(t) \\ X_v(t) \end{pmatrix}.$$

The dynamics of $\mathbf{x}(t)$ is obtained from (2)–(4). Linearizing around E_0^d (i.e., replacing $X_u(t)$ and $X_B(t)$ by their DFE values), we obtain

$$\begin{aligned}
\dot{X}_l(t) &= (1-\alpha)\beta \frac{\Lambda_u}{d_u} \int_0^{\omega_1} \Pi_1(\tau) X_v(t-\tau)\, d\tau - (\nu + d_l) X_l(t), \\
\dot{X}_i(t) &= \alpha\beta \frac{\Lambda_u}{d_u} \int_0^{\omega_2} \Pi_2(\tau) X_v(t-\tau)\, d\tau + \nu \int_0^{\omega_3} \Pi_3(\tau) X_l(t-\tau)\, d\tau - d_i X_i(t), \\
\dot{X}_v(t) &= r_v \int_0^{\omega_4} \Pi_4(\tau) X_i(t-\tau)\, d\tau - \left(d_v + \eta \frac{\Lambda_B}{d_B} \right) X_v(t).
\end{aligned}$$

The above system is a linear system with distributed delays of convolution type. It can be written abstractly as

$$\dot{\mathbf{x}}(t) = \mathcal{F}(\mathbf{x}_t) - \mathcal{V}(\mathbf{x}(t)),$$

where $\mathcal{F}$ contains the *new infection terms* (with delays), and $\mathcal{V}$ contains transition and removal terms.

Crucially, the delay terms represent the probability that an individual survives the delay period and contributes to infection at time t. Indeed, each kernel has the form

$$\Pi_i(\tau) = \zeta_i(\tau) e^{-n_i \tau},$$

so that $\Pi_i(\tau) d\tau$ is the probability density that the transition occurs after a delay τ with survival.

To compute the basic reproduction number, we consider exponential solutions of the form $e^{\lambda t}$. Substituting $X_j(t-\tau) = e^{-\lambda\tau} X_j(t)$, the delay integrals become Laplace transforms:

$$\int_0^{\omega_i} \Pi_i(\tau) e^{-\lambda\tau} d\tau.$$

At the threshold ($\lambda = 0$), these reduce to

$$F_i = \int_0^{\omega_i} \Pi_i(\tau)\, d\tau.$$

Thus, at the invasion threshold, each delayed transition contributes a factor F_i, which represents the *expected survival through the delay period*.

Using the above reduction, the linearized system becomes equivalent (at threshold) to the following ODE system:

$$\dot{\mathbf{x}} = (\mathbf{F_d} - \mathbf{V_d})\mathbf{x},$$

where

$$\mathbf{F_d} = \begin{pmatrix} 0 & 0 & (1-\alpha)\beta\dfrac{\Lambda_u}{d_u}F_1 \\ 0 & 0 & \alpha\beta\dfrac{\Lambda_u}{d_u}F_2 \\ 0 & 0 & 0 \end{pmatrix}, \quad \mathbf{V_d} = \begin{pmatrix} \nu + d_l & 0 & 0 \\ -\nu F_3 & d_i & 0 \\ 0 & -r_v F_4 & d_v + \eta\dfrac{\Lambda_B}{d_B} \end{pmatrix}.$$

Here,

- $\mathbf{F_d}$ collects *new infection terms*,
- $\mathbf{V_d}$ describes transitions and removals (including delayed transitions weighted by F_i).

The delayed basic reproduction number is defined as the spectral radius of the next-generation matrix:

$$R_0^d = \rho(\mathbf{F_d}\mathbf{V_d}^{-1}).$$

After explicit computation, this yields

$$\mathcal{R}_0^d = \frac{\Lambda_u r_v \beta d_B F_4\big(\alpha F_2(\nu + d_l) + F_1 F_3 \nu(1-\alpha)\big)}{d_i d_u (d_v d_B + \eta\Lambda_B)(\nu + d_l)}.$$

Each factor F_i arises rigorously from the Laplace transform of the delay kernel evaluated at $\lambda = 0$ and represents the probability that an individual:

- Survives the delay,
- Successfully contributes to the next infection stage.

Thus, the distributed-delay system induces a natural modification of the next-generation matrix, where each infection pathway is weighted by the corresponding survival probability through delays.

The Lemma 4 systematically analyzes the resulting algebraic system, distinguishing between the infection-free and endemic cases. We demonstrate that a unique endemic equilibrium emerges if and only if the delay-dependent reproduction number $\mathcal{R}_0^d$ exceeds unity, mirroring the threshold behavior observed in the non-delayed case.

Lemma 4.

- *Dynamics (1)–(5) admits an infection-free equilibrium* $\mathcal{E}_0^d = \left(\frac{\Lambda_u}{d_u}, 0, 0, 0, \frac{\Lambda_B}{d_B}\right)$.
- *If* $\mathcal{R}_0^d > 1$, *then dynamics (1)–(5) admits a unique endemic equilibrium* $\mathcal{E}_*^d = \left(X_u^*, X_l^*, X_i^*, X_v^*, X_B^*\right)$.

Proof. Note that for an equilibrium, all time derivatives are zero and state variables are constant. Substituting constants X_u, X_l, X_i, X_v, X_B into the integral terms gives:

$$\int_0^{\omega_i} \Pi_i(\tau) X(t-\tau) d\tau = X \int_0^{\omega_i} \Pi_i(\tau) d\tau = X F_i,$$

which holds because $X(t-\tau) = X$ (constant). Thus the equilibrium equations become algebraic and the factors F_i appear naturally.

The existence of equilibria for the distributed-delay system is established by solving the steady-state equations derived from setting the time derivatives in (1)–(5) to zero.

$$\begin{aligned}
0 &= \Lambda_u - d_u X_u - \beta X_u X_v, \\
0 &= (1-\alpha)F_1\beta X_u X_v - \nu X_l - d_l X_l, \\
0 &= \alpha F_2 \beta X_u X_v + \nu F_3 X_l - d_i X_i, \\
0 &= r_v F_4 X_i - d_v X_v - \eta X_v X_B, \\
0 &= \Lambda_B + \varepsilon X_v X_B - d_B X_B.
\end{aligned}$$

We find that the given model (1)–(5) admits two equilibria:

1. Infection-free equilibrium, $\mathcal{E}_0^d = \left(\frac{\Lambda_u}{d_u}, 0, 0, 0, \frac{\Lambda_B}{d_B}\right)$.
2. An endemic equilibrium, $\mathcal{E}_d^* = \left(X_u^*, X_l^*, X_i^*, X_v^*, X_B^*\right)$, where

$$X_u^* = \frac{(\nu + d_l)X_l^*}{(1-\alpha)F_1\beta X_v^*}, \; X_l^* = \frac{d_i F_1 (1-\alpha) X_i^*}{\alpha F_2(\nu + d_l) + F_1 F_3 \nu (1-\alpha)}, \; X_i^* = \frac{d_v X_v^* + \eta X_v^* X_B^*}{r_v F_4},$$
$$X_B^* = \frac{\Lambda_B}{d_B - \varepsilon X_v^*}.$$

where X_v^* satisfies the following equation:

$$\frac{b_2 X_v^2 + b_1 X_v + b_0}{d_B - \varepsilon X_v} = 0, \quad X_v \in \left(0, \frac{d_B}{\varepsilon}\right),$$

where

$$\begin{aligned}
b_2 &= d_i d_v \beta \varepsilon (\nu + d_l), \\
b_1 &= d_i d_u d_v \varepsilon (\nu + d_l) - d_i d_v \beta d_B (\nu + d_l) - d_i \eta \Lambda_B \beta (\nu + d_l) - \Lambda_u r_v \beta \varepsilon F_4 (\alpha F_2 (\nu + d_l) \\
&\quad + F_1 F_3 \nu (1-\alpha)), \\
b_0 &= \Lambda_u r_v \beta d_B F_4 (\alpha F_2 (\nu + d_l) + F_1 F_3 \nu (1-\alpha)) - d_i d_u d_v d_B (\nu + d_l) - d_i d_u \eta \Lambda_B (\nu + d_l).
\end{aligned}$$

Let us define a function $G(X_v)$ as $G(X_v) = b_2 X_v^2 + b_1 X_v + b_0, \quad X_v \in \left(0, \frac{d_B}{\varepsilon}\right)$. Function $G(X_v)$ is continuous on $X_v \in \left(0, \frac{d_B}{\varepsilon}\right)$. Then, we have

$$G(0) = d_i d_u (\nu + d_l)(\eta \Lambda_B + d_v d_B)(\mathcal{R}_0^d - 1) > 0, \quad \text{if } \mathcal{R}_0^d > 1,$$

and $G\left(\frac{d_B}{\varepsilon}\right) < 0$. Similarly to the proof of Lemma 2, $G(0) > 0$ if $\mathcal{R}_0^d > 1$ as well as $G\left(\frac{d_B}{\varepsilon}\right) < 0$. Since G is continuous on $\left[0, \frac{d_B}{\varepsilon}\right]$, the intermediate value theorem ensures the existence of at least one $X_v^* \in \left(0, \frac{d_B}{\varepsilon}\right)$ such that $G(X_v^*) = 0$.

Since $a_1 > 0$, the function G is strictly convex, and therefore it can have at most two real roots. Moreover, its derivative is $G'(X) = 2a_1 X + a_2$, which is strictly increasing on $\mathbb{R}$.

Assume, for contradiction, that Φ admits two distinct positive roots $0 < X_1 < X_2$. Then, by Rolle's theorem, there exists $c \in (X_1, X_2)$ such that $G'(c) = 0$. Since G' is strictly increasing, it has exactly one zero, given by $X_{\min} = -\frac{a_2}{2a_1}$. Thus, G decreases on $(-\infty, X_{\min})$ and increases on $(X_{\min}, +\infty)$.

Now, since $G(0) > 0$ and $G\left(\frac{d_B}{\varepsilon}\right) < 0$, the function must be strictly decreasing at least on an interval starting from 0, which implies $X_{\min} > 0$. Therefore, G is strictly decreasing on $(0, X_{\min})$ and strictly increasing on $(X_{\min}, +\infty)$. This implies that G can cross the horizontal axis at most once in $(0, X_{\min})$ and at most once in $(X_{\min}, +\infty)$. However, since

$$G(0) > 0 \quad \text{and} \quad G\left(\frac{d_B}{\varepsilon}\right) < 0,$$

the sign change occurs before reaching the minimum point $X_{\min}$. Hence, the root lies in the strictly decreasing region $(0, X_{\min})$. Consequently, G can admit only one root in the interval $\left(0, \frac{d_B}{\varepsilon}\right)$. Thus, there exists a unique X_v^* such that $0 < X_v^* < \frac{d_B}{\varepsilon}$ satisfies $G(X_v^*) = 0$. As a result, we get $X_u^* > 0$, $X_l^* > 0$, $X_i^* > 0$ and $X_B^* > 0$. This provides the existence and uniqueness of the endemic equilibrium $\mathcal{E}_*^d$ once $\mathcal{R}_0^d > 1$.

□

4.3. Global Stability

This subsection is devoted to establishing the global asymptotic stability properties of the equilibria for the distributed-delay HIV model (1)–(5). We construct explicit Lyapunov functionals that incorporate integral terms to account for the distributed delays, thereby extending the Lyapunov function techniques [32] used in the non-delayed case. For the infection-free equilibrium $\mathcal{E}_0^d$, we prove that it is globally asymptotically stable (GAS) whenever $\mathcal{R}_0^d \leq 1$, implying that the infection will be cleared from the host regardless of the initial viral load if the basic reproduction number is at or below the critical threshold. Conversely, when $\mathcal{R}_0^d > 1$, we demonstrate that the unique endemic equilibrium $\mathcal{E}_*^d$ is GAS, ensuring convergence to a chronic infection state for all positive initial conditions. The proofs rely on the construction of carefully chosen Lyapunov functionals that include memory terms capturing the delay history, and the application of LaSalle's Invariance Principle [32] for delay systems. These results confirm that the qualitative threshold behavior—where the dynamics are governed solely by $\mathcal{R}_0^d$—persists even in the presence of distributed delays, with no emergence of bistability or sustained oscillations. The analysis thus provides a foundation for understanding how biological latencies influence the long-term fate of the infection without altering the fundamental eradication-persistence dichotomy.

Let us define the number $K = \alpha F_2(\nu + d_l) + F_1 F_3 \nu(1-\alpha)$. Note that $\mathcal{R}_0^d = \frac{\Lambda_u r_v \beta d_B F_4 K}{d_i d_u (d_v d_B + \eta \Lambda_B)(\nu + d_l)}$.

Theorem 3. *The system (1)–(5) is globally asymptotically stable (GAS) around the infection-free equilibrium $\mathcal{E}_0^d$ if $\mathcal{R}_0^d \leq 1$.*

Proof. The proof is based on the Lyapunov function $\mathcal{F}_0^d(X_u, X_l, X_i, X_v, X_B)$ given by

$$\begin{aligned}
\mathcal{F}_0^d &= K\frac{\Lambda_u}{d_u} H\left(\frac{d_u X_u}{\Lambda_u}\right) + \nu F_3 X_l + (\nu + d_l) X_i + \frac{d_i(\nu + d_l)}{r_v F_4} X_v + \frac{d_i \eta(\nu + d_l)}{r_v \varepsilon F_4} \frac{\Lambda_B}{d_B} H\left(\frac{d_B X_B}{\Lambda_B}\right) \\
&+ \nu\beta(1-\alpha)F_3 \int_0^{\omega_1} \Pi_1(\tau) \int_{t-\tau}^{t} X_u(\theta) X_v(\theta)\, d\theta d\tau \\
&+ \alpha\beta(\nu + d_l) \int_0^{\omega_2} \Pi_2(\tau) \int_{t-\tau}^{t} X_u(\theta) X_v(\theta)\, d\theta d\tau \\
&+ \nu(\nu + d_l) \int_0^{\omega_3} \Pi_3(\tau) \int_{t-\tau}^{t} X_l(\theta)\, d\theta d\tau + \frac{d_i(\nu + d_l)}{F_4} \int_0^{\omega_4} \Pi_4(\tau) \int_{t-\tau}^{t} X_i(\theta)\, d\theta d\tau.
\end{aligned}$$

and by using the Lyapunov–LaSalle asymptotic stability theorem [32] to prove that $\mathcal{E}_0^d$ is GAS if $\mathcal{R}_0^d \leq 1$. More details are given in Appendix B.1. □

Theorem 4. *The system (1)–(5) is GAS around the endemic equilibrium $\mathcal{E}_d^*$ once $\mathcal{R}_0^d > 1$.*

Proof. The proof is based on the Lyapunov function $\mathcal{F}_d^*(X_u, X_l, X_i, X_v, X_B)$ given by

$$\begin{aligned}\mathcal{F}_d^* &= KX_u^* H\left(\frac{X_u}{X_u^*}\right) + \nu F_3 X_l^* H\left(\frac{X_l}{X_l^*}\right) + (\nu + d_l) X_i^* H\left(\frac{X_i}{X_i^*}\right) + \frac{d_i(\nu + d_l)}{r_v F_4} X_v^* H\left(\frac{X_v}{X_v^*}\right) \\ &+ \frac{d_i \eta (\nu + d_l)}{r_v \varepsilon F_4} X_B^* H\left(\frac{X_B}{X_B^*}\right) + \nu\beta(1-\alpha) F_3 X_u^* X_v^* \int_0^{\omega_1} \Pi_1(\tau) \int_{t-\tau}^{t} H\left(\frac{X_u(\theta) X_v(\theta)}{X_u^* X_v^*}\right) d\theta d\tau \\ &+ \alpha\beta(\nu + d_l) X_u^* X_v^* \int_0^{\omega_2} \Pi_2(\tau) \int_{t-\tau}^{t} H\left(\frac{X_u(\theta) X_v(\theta)}{X_u^* X_v^*}\right) d\theta d\tau \\ &+ \nu(\nu + d_l) X_l^* \int_0^{\omega_3} \Pi_3(\tau) \int_{t-\tau}^{t} H\left(\frac{X_l(\theta)}{X_l^*}\right) d\theta d\tau \\ &+ \frac{d_i(\nu + d_l)}{F_4} X_i^* \int_0^{\omega_4} \Pi_4(\tau) \int_{t-\tau}^{t} H\left(\frac{X_i(\theta)}{X_i^*}\right) d\theta d\tau.\end{aligned}$$

and by using the Lyapunov–LaSalle asymptotic stability theorem [32] to prove that $\mathcal{E}_d^*$ is GAS if $\mathcal{R}_0^d > 1$. More details are given in Appendix B.2. □

In conclusion, Section 4 has successfully extended the analytical framework of the within-host HIV model to incorporate distributed time delays, reflecting essential biological latencies in infection and immune response processes. We established the well-posedness of the delay system by proving the non-negativity and ultimate boundedness of solutions, confining the dynamics to a biologically meaningful invariant region. The generalized basic reproduction number $\mathcal{R}_0^d$ was derived, explicitly incorporating delay kernels through integral factors F_i, and shown to govern a sharp threshold for infection persistence. Using carefully constructed Lyapunov functionals that account for the delay history, we proved the global asymptotic stability of the infection-free equilibrium when $\mathcal{R}_0^d \leq 1$ and of the endemic equilibrium when $\mathcal{R}_0^d > 1$. These results demonstrate that although distributed delays quantitatively alter the threshold condition and system dynamics—by reducing $\mathcal{R}_0^d$ through the factors $F_i \leq 1$—they do not change the fundamental qualitative behavior: the system still exhibits a transcritical bifurcation at $\mathcal{R}_0^d = 1$, with no introduction of bistability or persistent oscillations. This analysis provides a robust theoretical foundation for understanding the impact of biological time lags on HIV dynamics and sets the stage for the numerical exploration of sensitivity, treatment effects, and delay-induced critical thresholds in Section 5.

5. Numerical Results and Discussion

This section presents a numerical investigation of the distributed-delay HIV model to illustrate the analytical results derived in previous sections and to explore the quantitative impact of key biological and pharmacological factors. We begin by specifying the delay structure, choosing the Dirac delta function $\delta(\tau - \tau_i)$ as a particular probability density, which reduces the general distributed-delay system to a discrete-delay model as the one given in [28] with fixed delays τ_i and survival probabilities $e^{-n_i \tau_i}$. Using a biologically plausible set of parameter values (Table 3), we perform numerical simulations to validate the stability theorems: first, by selecting parameters such that $\mathcal{R}_0^d < 1$ and demonstrating convergence to the infection-free equilibrium $\mathcal{E}_0^d$; and second, by increasing infection rates to achieve $\mathcal{R}_0^d > 1$ and showing convergence to the endemic equilibrium $\mathcal{E}_*^d$. We then conduct a detailed sensitivity analysis of $\mathcal{R}_0^d$, deriving and computing normalized sensitivity indices to rank parameters by their influence on the basic reproduction number. This analysis identifies the most effective targets for intervention. Furthermore, we examine the dynamics under antiretroviral treatment by incorporating an efficacy parameter κ, deriving the treatment-dependent reproduction number $\mathcal{R}_0^{\text{treatment}}(\kappa)$ and determining the critical drug efficacy κ^{cr} required for viral eradication. Finally, we investigate the specific

impact of the intracellular production delay τ_4 on the threshold condition, computing the critical delay τ_4^{cr} that suppresses the infection. Together, these numerical explorations bridge the theoretical analysis with practical insights, highlighting how delays, treatment, and parameter variations shape the within-host dynamics of HIV.

By choosing the Dirac delta function $\delta(\cdot)$ as a specific form of the probability distribution, we define $\zeta_i(\tau) = \delta(\tau - \tau_i), i = 1, \cdots, 4$. In case $\omega_i = \infty, i = 1, \cdots, 4$, we get $\int_0^\infty \zeta_i(\tau)d\tau = 1$, and $F_i = \int_0^\infty \delta(\tau - \tau_i)e^{-\eta_i\tau}d\tau = e^{-\eta_i\tau_i}, i = 1, \cdots, 4$. Then,

$$\begin{aligned}
&\int_0^\infty \delta(\tau - \tau_1)e^{-n_1\tau}X_u(t-\tau)X_v(t-\tau)\,d\tau = e^{-n_1\tau_1}X_u(t-\tau_1)X_v(t-\tau_1),\\
&\int_0^\infty \delta(\tau - \tau_2)e^{-n_2\tau}X_u(t-\tau)X_v(t-\tau)\,d\tau = e^{-n_2\tau_2}X_u(t-\tau_2)X_v(t-\tau_2),\\
&\int_0^\infty \delta(\tau - \tau_3)e^{-n_3\tau}X_l(t-\tau)\,d\tau = e^{-n_3\tau_3}X_l(t-\tau_3),\\
&\int_0^\infty \delta(\tau - \tau_4)e^{-n_4\tau}X_i(t-\tau)\,d\tau = e^{-n_4\tau_4}X_i(t-\tau_4).
\end{aligned}$$

Hence, model (1)–(5) can be written as

$$\begin{aligned}
\dot{X}_u(t) &= \Lambda_u - d_uX_u(t) - \beta X_u(t)X_v(t),\\
\dot{X}_l(t) &= (1-\alpha)\beta e^{-n_1\tau_1}X_u(t-\tau_1)X_v(t-\tau_1) - (\nu + d_l)X_l(t),\\
\dot{X}_i(t) &= \alpha\beta e^{-n_2\tau_2}X_u(t-\tau_2)X_v(t-\tau_2) + \nu e^{-n_3\tau_3}X_l(t-\tau_3) - d_iX_i(t),\\
\dot{X}_v(t) &= r_v e^{-n_4\tau_4}X_i(t-\tau_4) - d_vX_v(t) - \eta X_v(t)X_B(t),\\
\dot{X}_B(t) &= \Lambda_B + \varepsilon X_v(t)X_B(t) - d_BX_B(t),
\end{aligned} \tag{12}$$

for all $t > 0$ where the initial values are picked as constants functions on $[-\tau^*, 0]$. For simplicity, in all numerical simulations, we choose the delay parameters as $\tau_1 = \tau_2 = \tau_3 = \tau_4 = 0.1$.

The basic reproduction number of model (12) is given by:

$$\mathcal{R}_0^d = \frac{\Lambda_u r_v \beta d_B\left(\alpha e^{-n_2\tau_2}(\nu + d_l) + e^{-(n_1\tau_1 + n_3\tau_3)}\nu(1-\alpha)\right)e^{-n_4\tau_4}}{d_u d_i(d_v d_B + \eta\Lambda_B)(\nu + d_l)}.$$

Table 3. Numerical values of the model parameters that are derived from the cited sources. β and τ_i are varied.

Symbol	Value	Source
Λ_u	10 cells mm^{-3} day^{-1}	[14,39]
d_u	0.01 day^{-1}	[40,41]
d_i	0.4 day^{-1}	[39]
r_v	38 viruses cells^{-1} day^{-1}	[41,42]
d_v	2.4 day^{-1}	[14,39,41]
η	0.1 cells^{-1} mm^3 day^{-1}	
Λ_B	48 cells mm^{-3} day^{-1}	[43]
ε	0.01 viruses^{-1} mm^3 day^{-1}	[44]
d_B	0.24 day^{-1}	[43]
α	0.1	[45]
ν	0.01 day^{-1}	[45]
d_l	0.04 day^{-1}	[45]
n_i	1 day^{-1}	[46,47]

5.1. Validation of Global Stability

This subsection provides numerical validation of the global stability theorems established in Sections 3 and 4 by simulating the dynamics of the discrete-delay HIV model given by system (12). Using the baseline parameter values from Table 3 with $\tau_1 = \tau_2 = \tau_3 = \tau_4 = 0.1$, we select two distinct incidence rates (β) to illustrate the threshold behavior governed by the basic reproduction number $\mathcal{R}_0^d$. Note that our aim is qualitative validation of analytical stability results, not quantitative clinical prediction; nonetheless, the parameters lie within physiologically plausible ranges.

First, with infection rate $\beta = 0.0002$, we obtain $\mathcal{R}_0^d = 0.47 < 1$, confirming that the infection-free equilibrium $\mathcal{E}_0^d$ is globally asymptotically stable (GAS). Simulations of all compartment trajectories, uninfected CD4$^+$ T cells, latently infected cells, actively infected cells, free virions, and B cells demonstrate clear convergence to $\mathcal{E}_0^d = \left(\frac{\Lambda_u}{d_u}, 0, 0, 0, \frac{\Lambda_B}{d_B}\right)$, as shown in Figure 2. Second, by increasing the infection rate to $\beta = 0.0008$, we obtain $\mathcal{R}_0^d = 1.89 > 1$, which ensures the existence and global stability of the unique endemic equilibrium $\mathcal{E}_*^d$. Corresponding simulations (Figure 3) show convergence of all state variables to positive steady-state values, illustrating the establishment of a chronic infection. These numerical results not only corroborate the analytical stability proofs but also visually demonstrate the sharp threshold dynamics: the system transitions from viral clearance to persistent infection precisely as $\mathcal{R}_0^d$ crosses unity. The simulations were performed using standard delay differential equation solvers with biologically consistent initial conditions, further confirming the model's robustness and the practical relevance of the theoretical threshold.

Figure 2 demonstrates convergence of all compartment trajectories to $\mathcal{E}_0^d = \left(\frac{\Lambda_u}{d_u}, 0, 0, 0, \frac{\Lambda_B}{d_B}\right)$. This confirms the theoretical result that when $\mathcal{R}_0^d \leq 1$, the infection is cleared and the system returns to a healthy state regardless of initial viral load. Figure 3 shows trajectories converging to positive steady-state values, illustrating the establishment of a chronic infection. It validates the analytical prediction that a unique endemic equilibrium exists and is globally stable when $\mathcal{R}_0^d > 1$.

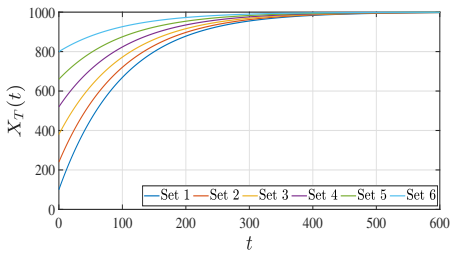

(**a**) Uninfected CD4$^+$ T cells

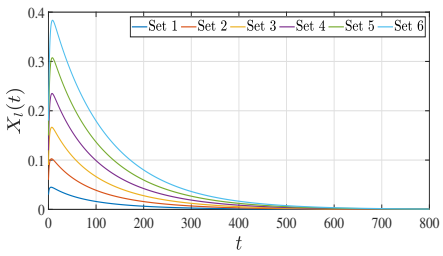

(**b**) Latently infected CD4$^+$ T cells

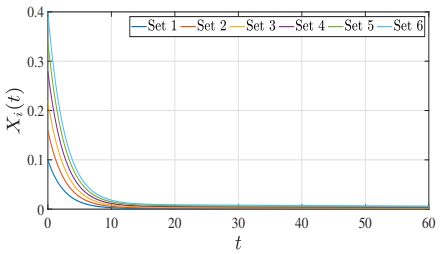

(**c**) Actively infected CD4$^+$ T cells

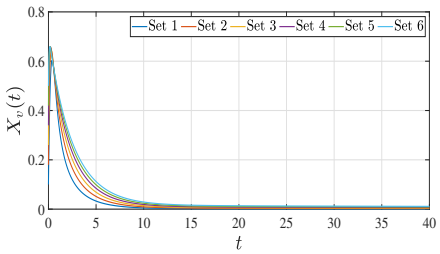

(**d**) Free virions

Figure 2. *Cont.*

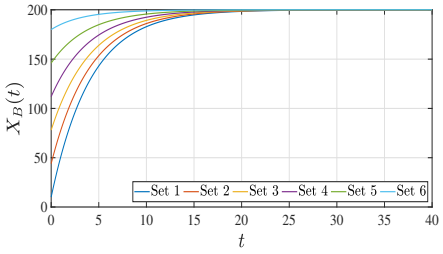

(**e**) B cells

Figure 2. Time series of the model variables for different constant history values (see Table 2). Each color corresponds to one set of initial history values listed in Table 4. For $\beta = 0.0002$, we get $\mathcal{R}_0^d = 0.47 < 1$, therefore, $\mathcal{E}_0^d$ is GAS.

Table 4. Sets of constant initial history values of $(X_u(\theta), X_l(\theta), X_i(\theta), X_v(\theta), X_B(\theta))$ for $\theta \in [-\tau_{\max}, 0] = [-0.1, 0]$ used for Figure 2.

Variable	Set 1	Set 2	Set 3	Set 4	Set 5	Set 6
$X_u(\theta)$	100	240	380	520	660	800
$X_l(\theta)$	0.03	0.06	0.09	0.12	0.15	0.18
$X_i(\theta)$	0.1	0.16	0.22	0.28	0.34	0.4
$X_v(\theta)$	0.1	0.18	0.26	0.34	0.42	0.5
$X_B(\theta)$	10	44	78	112	146	180

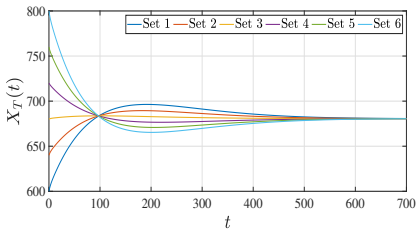

(**a**) Uninfected CD4$^+$ T cells

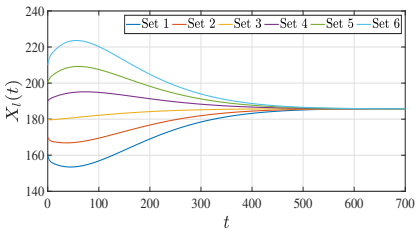

(**b**) Latently infected CD4$^+$ T cells

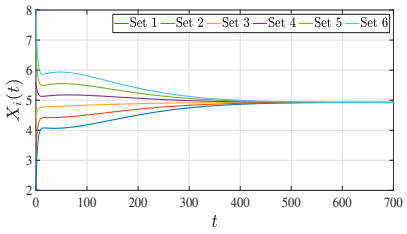

(**c**) Actively infected CD4$^+$ T cells

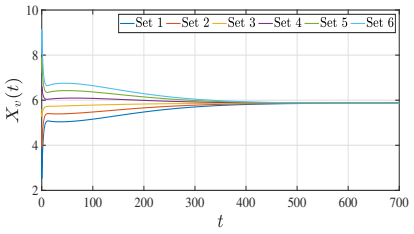

(**d**) Free virions

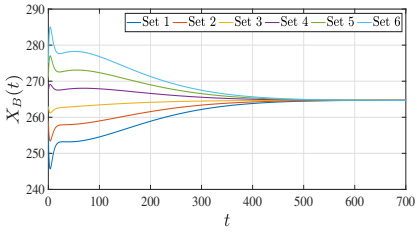

(**e**) B cells

Figure 3. Time series of the model variables for different constant history values (see Table 3). Each color corresponds to one set of initial history values listed in Table 5. For $\beta = 0.0008$, we get $\mathcal{R}_0^d = 1.89 > 1$; therefore, $\mathcal{E}_*^d$ is GAS.

Table 5. Sets of constant history values of $(X_u(\theta), X_l(\theta), X_i(\theta), X_v(\theta), X_B(\theta))$ for $\theta \in [-\tau_{\max}, 0] = [-0.1, 0]$ used for Figure 3.

Variable	Set 1	Set 2	Set 3	Set 4	Set 5	Set 6
$X_u(\theta)$	600	640	680	720	760	800
$X_l(\theta)$	160	170	180	190	200	210
$X_i(\theta)$	2	3.2	4.4	5.6	6.8	8
$X_v(\theta)$	4	4.8	5.6	6.4	7.2	8
$X_B(\theta)$	255	259	263	267	271	275

5.2. Sensitivity Analysis of $\mathcal{R}_0^D$

To quantify how variations in individual model parameters influence the basic reproduction number $\mathcal{R}_0^d$, we perform a normalized forward sensitivity analysis [48,49]. The normalized sensitivity index (or elasticity) of $\mathcal{R}_0^d$ with respect to a parameter p is defined as $S_p = \dfrac{p}{\mathcal{R}_0^d} \cdot \dfrac{\partial \mathcal{R}_0^d}{\partial p}$.

The analytical expression for $\mathcal{R}_0^d$ is $\mathcal{R}_0^d = \dfrac{\Lambda_u r_v \beta d_B F_4 \left[\alpha F_2(\nu + d_l) + F_1 F_3 \nu(1-\alpha)\right]}{d_i d_u (d_v d_B + \eta \Lambda_B)(\nu + d_l)}$, where the delay factors are given by $F_i = \displaystyle\int_0^{\omega_i} \zeta_i(\tau) e^{-n_i \tau}\, d\tau$. The partial derivatives of $\mathcal{R}_0^d$ with respect to each parameter are computed, and the corresponding sensitivity indices are as follows:

- Parameters appearing linearly in the numerator:

$$S_{\Lambda_u} = 1, \qquad S_{r_v} = 1, \qquad S_\beta = 1.$$

- Parameters appearing linearly in the denominator:

$$S_{d_u} = -1, \qquad S_{d_i} = -1, \qquad S_{d_v} = -\frac{d_v d_B}{d_v d_B + \eta \Lambda_B},$$
$$S_{d_B} = \frac{d_B \eta \Lambda_B}{d_v d_B + \eta \Lambda_B}, \qquad S_\eta = -\frac{\eta \Lambda_B}{d_v d_B + \eta \Lambda_B}, \qquad S_{\Lambda_B} = -\frac{\eta \Lambda_B}{d_v d_B + \eta \Lambda_B}.$$

- Parameters in the activation term:

$$S_\nu = \frac{\nu}{\nu + d_l}\left[\frac{F_1 F_3 (1-\alpha)}{\alpha F_2 + F_1 F_3 \frac{\nu(1-\alpha)}{\nu + d_l}} - \frac{d_l}{\nu + d_l}\right],$$
$$S_{d_l} = -\frac{d_l}{\nu + d_l}\left[1 + \frac{\nu(1-\alpha) F_1 F_3}{\alpha F_2(\nu + d_l) + \nu(1-\alpha) F_1 F_3}\right].$$

- Parameters in the delay factors F_i:

$$S_{n_1} = -\frac{F_1 F_3 \nu (1-\alpha) n_1 \tau_1}{\alpha F_2(\nu + d_l) + F_1 F_3 \nu (1-\alpha)}, \quad S_{\tau_1} = -\frac{F_1 F_3 \nu (1-\alpha) n_1 \tau_1}{\alpha F_2(\nu + d_l) + F_1 F_3 \nu (1-\alpha)},$$
$$S_{n_2} = -\frac{\alpha F_2 (\nu + d_l) n_2 \tau_2}{\alpha F_2(\nu + d_l) + F_1 F_3 \nu (1-\alpha)}, \quad S_{\tau_2} = -\frac{\alpha F_2 (\nu + d_l) n_2 \tau_2}{\alpha F_2(\nu + d_l) + F_1 F_3 \nu (1-\alpha)},$$
$$S_{n_3} = -\frac{F_1 F_3 \nu (1-\alpha) n_3 \tau_3}{\alpha F_2(\nu + d_l) + F_1 F_3 \nu (1-\alpha)}, \quad S_{\tau_3} = -\frac{F_1 F_3 \nu (1-\alpha) n_3 \tau_3}{\alpha F_2(\nu + d_l) + F_1 F_3 \nu (1-\alpha)},$$
$$S_{n_4} = -n_4 \tau_4, \quad S_{\tau_4} = -n_4 \tau_4.$$

Numerical Sensitivity Ranking

Using the baseline parameter values from Table 3 with $\tau_1 = \tau_2 = \tau_3 = \tau_4 = 0.1$, the computed sensitivity indices are as shown below in Figure 4 and Table 6.

Table 6. Numerical sensitivity indices for $\mathcal{R}_0^d$ (baseline parameters).

Parameter p	Λ_u	r_v	β	ν	d_B	n_2, τ_2	n_1, τ_1	
Sensitivity Index S_p	+1	+1	+1	+0.649	+0.214	−0.015	−0.085	
Parameter p	n_3, τ_3	d_v	n_4, τ_4	d_l	η	Λ_B	d_u	d_i
Sensitivity Index S_p	−0.085	−0.107	−0.1	−0.53	−0.893	−0.893	−1	−1

The bar chart in Figure 4 displays normalized sensitivity indices (S_p) for each parameter, quantifying their relative influence on $\mathcal{R}_0^d$. Positive values (e.g., Λ_u, r_v, β, ν) indicate that increasing the parameter raises $\mathcal{R}_0^d$, while negative values (e.g., d_i, d_u, Λ_B, η, d_l, delay-related parameters) signify a reducing effect. This visualization helps identify priority targets for intervention.

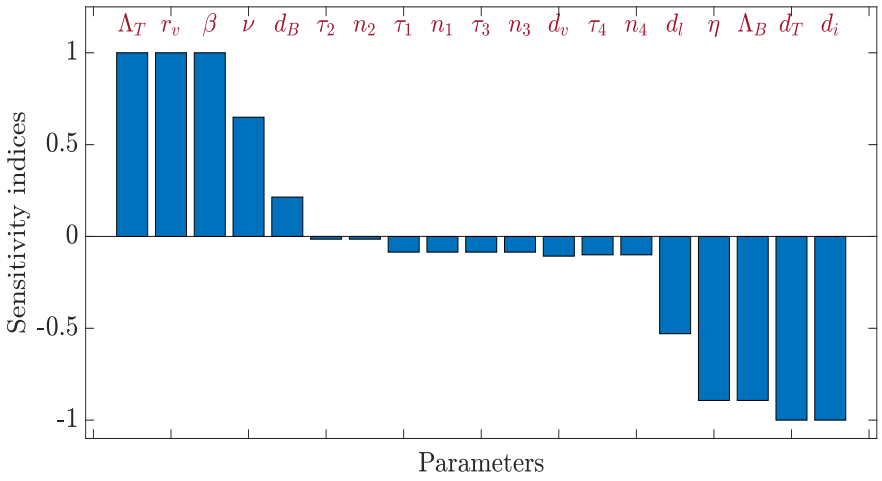

Figure 4. Sensitivity analysis for $\mathcal{R}_0^d$.

5.3. Treatment Effects

Drugs such as zidovudine (AZT), tenofovir, and emtricitabine inhibit the reverse transcription of viral RNA into DNA, thereby blocking new infections. In our model, this is represented by reducing the infection rate β by a factor $(1 - \kappa)$, where $\kappa \in [0, 1]$ represents drug efficacy:

$$\beta_{\text{eff}} = (1 - \kappa)\beta. \tag{13}$$

Clinical studies by Deeks et al. [50] report that RTIs typically achieve 70-90% inhibition of viral replication when used as monotherapy, and 90-95% when combined with other agents. The efficacy parameter κ can be interpreted as the fraction of reverse transcription events that are successfully blocked.

The corresponding basic reproduction number under treatment, $\mathcal{R}_0^{\text{treatment}}(\kappa) = (1 - \kappa)\mathcal{R}_0^d$, decreases linearly with increasing drug efficacy, directly linking pharmacological intervention to the infection threshold. We derive the critical drug efficacy $\kappa^{\text{cr}} = 1 - 1/\mathcal{R}_0^d$, which represents the minimum treatment effectiveness required to reduce $\mathcal{R}_0^{\text{treatment}}(\kappa)$ below unity and ensure viral eradication. Using numerical simulations, we explore how varying κ influences the system's long-term behavior. Table 7 summarizes the values of $\mathcal{R}_0^{\text{treatment}}(\kappa)$ for different efficacies, illustrating the transition from endemic persistence

($\kappa < \kappa^{cr}$) to infection clearance ($\kappa \geq \kappa^{cr}$). Figure 5 visually demonstrates this transition by plotting compartment trajectories for representative κ values, showing how effective treatment suppresses viral load and enables immune recovery. These results highlight the critical role of treatment adherence and efficacy in achieving undetectable viral loads and provide a quantitative framework for assessing the necessary intervention intensity to shift the system from chronic infection to a disease-free state.

The model in the presence of treatment with an efficacy parameter $\kappa \in [0,1]$ is given as follows:

$$\begin{aligned}
\dot{X}_u(t) &= \Lambda_u - d_u X_u(t) - (1-\kappa)\beta X_u(t) X_v(t),\\
\dot{X}_l(t) &= (1-\alpha)(1-\kappa)\beta e^{-n_1\tau_1} X_u(t-\tau_1) X_v(t-\tau_1) - (\nu + d_l) X_l(t),\\
\dot{X}_i(t) &= \alpha(1-\kappa)\beta e^{-n_2\tau_2} X_u(t-\tau_2) X_v(t-\tau_2) + \nu e^{-n_3\tau_3} X_l(t-\tau_3) - d_i X_i(t),\\
\dot{X}_v(t) &= r_v e^{-n_4\tau_4} X_i(t-\tau_4) - d_v X_v(t) - \eta X_v(t) X_B(t),\\
\dot{X}_B(t) &= \Lambda_B + \varepsilon X_v(t) X_B(t) - d_B X_B(t),
\end{aligned} \tag{14}$$

for all $t > 0$ where the initial values are picked as constant functions on $[-\tau^*, 0]$.

The basic reproduction number in the presence of treatment can be expressed as follows: $\mathcal{R}_0^{\text{treatment}}(\kappa) = (1-\kappa)\mathcal{R}_0^d \leq \mathcal{R}_0^d$. The critical drug efficacy necessary for viral eradication is obtained by solving the following inequalities: $\kappa^{cr} = 1 - \dfrac{1}{\mathcal{R}_0^d}$ ensuring $\mathcal{R}_0^{\text{treatment}}(\kappa) \leq 1$ for all $\kappa \geq \kappa^{cr}$.

By using the baseline parameter values from Table 3 and fixing the parameters $\beta = 0.001$ and $\tau_1 = \tau_2 = \tau_3 = \tau_4 = 0.01$, and varying κ, we study the impact of drug efficacy, κ, on the stability of $\mathcal{E}_0^d$. The approximated critical value of κ^{cr} is given by $\kappa^{cr} \simeq 0.6734$. If $\kappa^{cr} \geq 0.6734$, then $\mathcal{R}_0^d(\kappa) \leq 1$, and the global stability of $\mathcal{E}_0^d$. However, if $\kappa^{cr} < 0.6734$, $\mathcal{R}_0^d(\kappa)$ exceeds 1, destabilizing $\mathcal{E}_0^d$.

Table 7. Impact of treatment efficacies κ on $\mathcal{R}_0^{\text{treatment}}(\kappa)$.

κ	**0.3**	**0.4**	**0.6734**	**0.8**	**0.9**
$R_0^{\text{treatment}}(\kappa)$	2.1431	1.8369	1	0.6123	0.3062

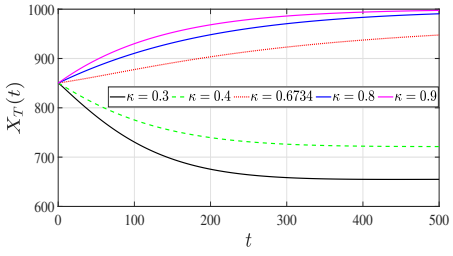

(**a**) Uninfected CD4$^+$ T cells

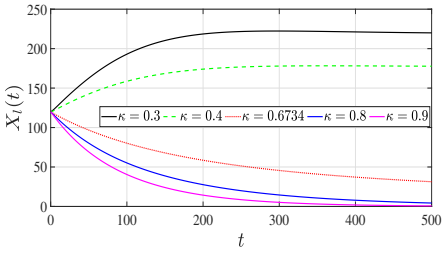

(**b**) Latently infected CD4$^+$ T cells

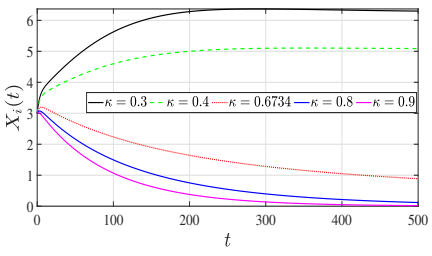

(**c**) Actively infected CD4$^+$ T cells

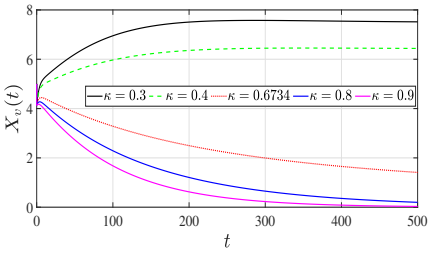

(**d**) Free virions

Figure 5. *Cont.*

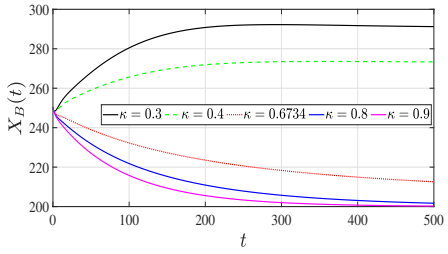

(**e**) B cells

Figure 5. Impact of treatment efficacies κ on the dynamics starting from the same constant initial history values $(X_u(\theta), X_l(\theta), X_i(\theta), X_v(\theta), X_B(\theta)) = (850, 120, 3, 5, 250)$ for $\theta \in [-\tau_{\max}, 0] = [-0.1, 0]$.

The plots in Figure 5 illustrate how varying levels of antiretroviral therapy affect viral load and immune cell populations. As κ increases, $\mathcal{R}_0^{\text{treatment}}(\kappa)$ decreases, leading to suppression of the virus and eventual convergence to the infection-free state when $\kappa \geq \kappa^{\text{cr}} = 0.6734$.

5.4. Delay Impact

This subsection examines the specific influence of the intracellular production delay τ_4, representing the time between active infection and virion release, on the infection threshold and long-term dynamics. The basic reproduction number $\mathcal{R}_0^d$ depends exponentially on τ_4 via the factor $e^{-n_4\tau_4}$, making this delay a critical modulator of infection persistence. We derive an explicit expression for the critical delay τ_4^{cr} by solving $\mathcal{R}_0^d(\tau_4) = 1$, yielding

$$\tau_4^{\text{cr}} = \max\left\{0,\ \frac{1}{n_4}\ln\left(\frac{\Lambda_u r_v \beta d_B\left[\alpha e^{-n_2\tau_2}(\nu + d_l) + e^{-n_1\tau_1 - n_3\tau_3}\nu(1-\alpha)\right]}{d_i d_u (d_v d_B + \eta\Lambda_B)(\nu + d_l)}\right)\right\}.$$

If $\tau_4 \geq \tau_4^{\text{cr}}$, then $\mathcal{R}_0^d \leq 1$ and the infection-free equilibrium is globally stable; conversely, if $\tau_4 < \tau_4^{\text{cr}}$, the endemic equilibrium prevails. Using baseline parameters, we compute $\tau_4^{\text{cr}} \approx 1.1289$ days. Figure 6 illustrates the effect of varying τ_4 on system trajectories, showing how increasing τ_4 progressively suppresses viral load and can eventually lead to infection clearance. This analysis underscores the potential role of delay-inducing therapeutic strategies, such as drugs that prolong the intracellular viral maturation phase, in pushing $\mathcal{R}_0^d$ below the critical threshold. It also highlights the sensitivity of the infection outcome to variations in this biological latency, providing insight into how natural or induced delays can fundamentally alter the course of HIV infection.

$$\mathcal{R}_0^d(\tau_4) = e^{-n_4\tau_4}\left(\frac{\Lambda_u r_v \beta d_B\left[\alpha e^{-n_2\tau_2}(\nu + d_l) + e^{-n_1\tau_1 - n_3\tau_3}\nu(1-\alpha)\right]}{d_i d_u (d_v d_B + \eta\Lambda_B)(\nu + d_l)}\right).$$

To guarantee that $\mathcal{R}_0^d(\tau_4) \leq 1$, we compute the critical values τ_4^{cr} as

$$\tau_4^{\text{cr}} = \max\left\{0, \frac{1}{n_4}\ln\left(\frac{\Lambda_u r_v \beta d_B\left[\alpha e^{-n_2\tau_2}(\nu + d_l) + e^{-n_1\tau_1 - n_3\tau_3}\nu(1-\alpha)\right]}{d_i d_u (d_v d_B + \eta\Lambda_B)(\nu + d_l)}\right)\right\}.$$

By using the baseline parameter values from Table 3, fixing the parameters $\beta = 0.001$ and $\tau_1 = \tau_2 = \tau_3 = 0.01$, and varying τ_4, we study the impact of the time delay, τ_4, on the stability of $\mathcal{E}_0^d$. The approximated critical value of τ_4^{cr} is given by $\tau_4^{\text{cr}} \simeq 1.1289$. If $\tau_4^{\text{cr}} \geq 1.1289$, then $\mathcal{R}_0^d(\tau_4) \leq 1$, and the global stability of $\mathcal{E}_0^d$. However, if $\tau_4^{\text{cr}} < 1.1289$, $\mathcal{R}_0^d(\tau_4)$ exceeds 1, destabilizing $\mathcal{E}_0^d$.

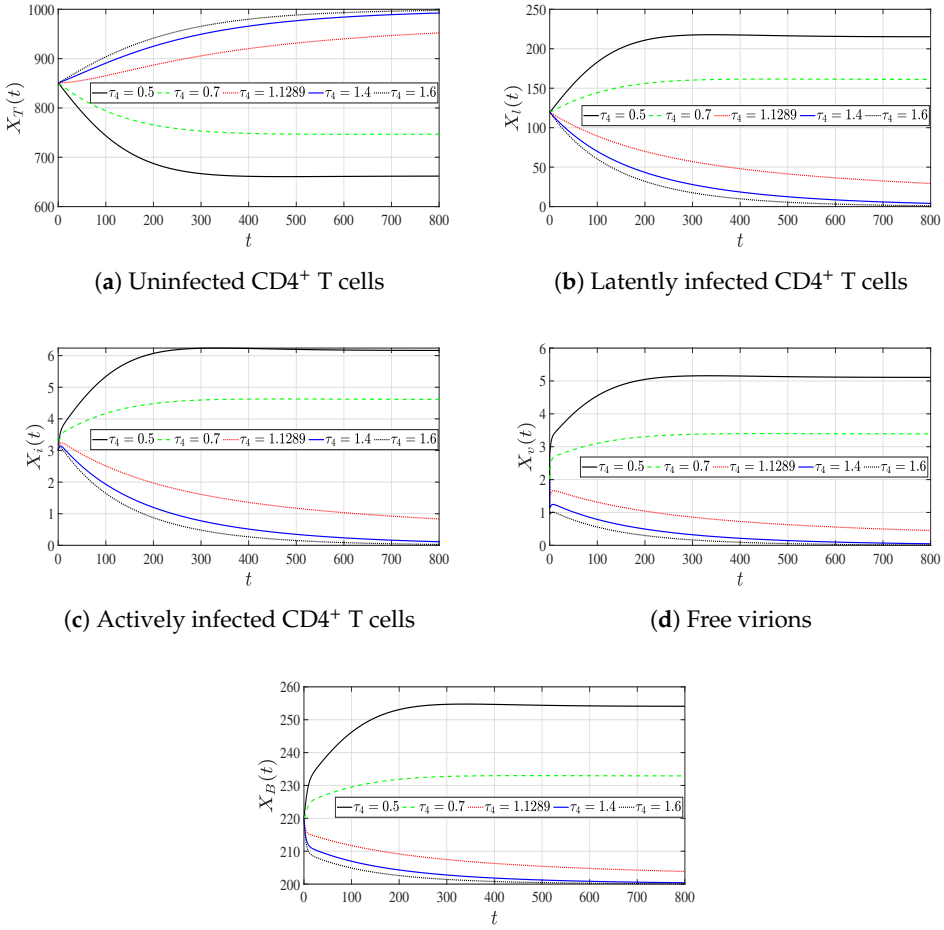

(**a**) Uninfected CD4$^+$ T cells

(**b**) Latently infected CD4$^+$ T cells

(**c**) Actively infected CD4$^+$ T cells

(**d**) Free virions

(**e**) B cells

Figure 6. Effect of the maturation delay τ_4 on system (7)–(11) starting from the same constant initial history values $(X_u(\theta), X_l(\theta), X_i(\theta), X_v(\theta), X_B(\theta)) = (850, 120, 3, 2, 220)$ for $\theta \in [-\tau_{\max}, 0] = [-0.1, 0]$.

Figure 6 and Table 8 show how increasing the intracellular production delay τ_4 reduces viral load and can shift the system from an endemic to an infection-free state when $\tau_4 \geq \tau_4^{\text{cr}}$. This highlights the potential therapeutic benefit of prolonging viral maturation.

Table 8. Effect of the maturation delay τ_4 on $\mathcal{R}_0^d(\tau_4)$.

τ_4	**0.5**	**0.7**	**1.1289**	**1.4**	**1.6**
$R_0^d(\tau_4)$	1.8756	1.5356	1	0.7626	0.6243

6. Conclusions

This paper presented a mathematical analysis of a within-host HIV infection model incorporating latent reservoirs, distributed time delays, and a B-cell-mediated immune response. The model, formulated as a system of nonlinear delay differential equations, captures essential biological features: time lags between viral entry and infected cell emergence, latent cell reactivation, intracellular viral production, and B-cell proliferation in response to viral stimulation.

The study established well-posedness by proving non-negativity and boundedness of solutions, identifying a positively invariant region. For the non-delayed system, the basic reproduction number $\mathcal{R}_0$ was derived, and a sharp threshold dynamic was proved using Lyapunov functions and LaSalle's Invariance Principle: the infection-free equilibrium is

globally asymptotically stable (GAS) when $\mathcal{R}_0 \leq 1$, while a unique endemic equilibrium is GAS when $\mathcal{R}_0 > 1$. These results were extended to the distributed-delay system, yielding a generalized reproduction number $\mathcal{R}_0^d$ incorporating delay kernel integrals F_i. The same threshold behavior persists: the infection-free equilibrium is GAS when $\mathcal{R}_0^d \leq 1$, and the endemic equilibrium is GAS when $\mathcal{R}_0^d > 1$, confirming that distributed delays quantitatively alter the threshold but do not introduce bistability or sustained oscillations.

Numerical simulations validated the analytical results. Sensitivity analysis identified the most influential parameters for intervention, including viral production rate r_v, recruitment rates Λ_u and Λ_B, infection rate β, neutralization rate η, and death rates d_u and d_i. Treatment effects were explored, showing that drug efficacy κ linearly reduces $\mathcal{R}_0^d$, with critical efficacy κ^{cr} derived for viral eradication. The intracellular delay τ_4 was shown to act as a critical threshold, where increasing τ_4 can suppress $\mathcal{R}_0^d$ below unity, highlighting potential delay-inducing therapeutic strategies.

The model has several limitations: linear incidence terms (may not capture all virus–cell and immune nonlinearities); absence of spatial heterogeneity, drug resistance mutations, and CTL dynamics; the need for precise biological forms of delay kernels; and inter-patient variability affecting quantitative generalizability. The B-cell proliferation term assumes purely stimulatory effects without incorporating potential HIV-induced B-cell impairment or exhaustion, representing a baseline scenario for future extension once more detailed biological data become available.

Several future directions emerge: first, incorporating drug-specific mechanisms (reverse transcriptase inhibitors, protease inhibitors) and pharmacokinetics would improve representation of combination ART; second, extending the model to include CTL responses and viral mutation dynamics would allow study of immune escape and long-term treatment failure; third, connecting within-host to between-host transmission dynamics could bridge individual-level pathogenesis to population-level epidemiology; fourth, validating the model with longitudinal clinical data would enable patient-specific parameter estimation; fifth, exploring optimal control strategies based on sensitivity analysis could inform personalized treatment schedules, minimizing viral load while limiting toxicity and resistance; sixth, determining whether the global stability results extend to saturated (Holling type II) or other nonlinear incidence functions—numerical simulations suggest persistence of threshold behavior, but rigorous Lyapunov construction is non-trivial. Seventh, the distributed-delay formulation connects naturally to survival analysis frameworks: delay kernels $\Pi_i(\tau) = \zeta_i(\tau)e^{-n_i\tau}$ can be interpreted as survival-weighted probability densities, and factors F_i correspond to cumulative survival probabilities. This opens the door to estimating delay parameters from clinical survival data using inverse Gaussian or other parametric survival models [51,52], with future work combining survival analysis with DDEs. Eighth, while the present analysis proves global stability for positive kernels, bifurcation phenomena may arise under alternative assumptions; a systematic bifurcation analysis is deferred to future work, investigating saturated incidence, gamma-distributed delays, oscillatory kernels, and numerical bifurcation continuation to map stability regions and possible periodic solutions.

In summary, this work provides a mathematical framework for understanding the roles of latency, distributed delays, and immune response in HIV dynamics, underscoring threshold-based approaches for predicting infection outcomes and identifying therapeutic avenues.

Author Contributions: Conceptualization, F.K.A., M.I.A., M.H.A. and M.E.H.; methodology, F.K.A., M.I.A., M.H.A. and M.E.H.; software, F.K.A., M.I.A., M.H.A. and M.E.H.; investigation, F.K.A., M.I.A., M.H.A. and M.E.H.; visualization, F.K.A., M.I.A., M.H.A. and M.E.H.; writing—original draft, F.K.A.,

M.I.A., M.H.A. and M.E.H.; writing—review and editing, F.K.A., M.I.A., M.H.A. and M.E.H. All authors have read and agreed to the published version of the manuscript.

Funding: This work was funded by the Deanship of Graduate Studies and Scientific Research at Najran University for funding this work under the Najran Research Funding Program, grant code (NU/CPL/SERC/14/2821-1).

Data Availability Statement: The original contributions presented in the study are included in the article. Further inquiries can be directed to the corresponding author.

Acknowledgments: The authors are thankful to the Deanship of Graduate Studies and Scientific Research at Najran University for funding this work under the Consortium Funding Program grant code (NU/CPL/SERC/14/2821-1). The authors are also grateful to the unknown referees for the many constructive suggestions, which helped to improve the presentation of the paper.

Conflicts of Interest: The authors declare no conflicts of interest.

Appendix A. Proof of Theorems 1 and 2

Appendix A.1. Proof of Theorem 1

Proof of Theorem 1. Assume that $\mathcal{R}_0 \leq 1$, and define the Lyapunov function $\mathcal{F}_0(X_u, X_l, X_i, X_v, X_B)$ as

$$\mathcal{F}_0 = \frac{\Lambda_u}{d_u} H\left(\frac{d_u X_u}{\Lambda_u}\right) + \frac{\nu}{\nu + d_l\alpha} X_l + \frac{\nu + d_l}{\nu + d_l\alpha} X_i + \frac{d_i(\nu + d_l)}{r_v(\nu + d_l\alpha)} X_v + \frac{d_i\eta(\nu + d_l)}{r_v\varepsilon(\nu + d_l\alpha)} \frac{\Lambda_B}{d_B} H\left(\frac{d_B X_B}{\Lambda_B}\right).$$

Clearly, $\mathcal{F}_0(X_u, X_l, X_i, X_v, X_B) > 0$ for any $X_u, X_l, X_i, X_v, X_B > 0$, and $\mathcal{F}_0(\frac{\Lambda_u}{d_u}, 0, 0, 0, \frac{\Lambda_B}{d_B}) = 0$. Calculate $\frac{d\mathcal{F}_0}{dt}$ along the solutions of model (7)–(11):

$$\begin{aligned}\frac{d\mathcal{F}_0}{dt} =& \left(1 - \frac{\Lambda_u}{d_u X_u}\right)\dot{X}_u + \frac{\nu}{\nu + d_l\alpha}\dot{X}_l + \frac{\nu + d_l}{\nu + d_l\alpha}\dot{X}_i + \frac{d_i(\nu + d_l)}{r_v(\nu + d_l\alpha)}\dot{X}_v \\ &+ \frac{d_i\eta(\nu + d_l)}{r_v\varepsilon(\nu + d_l\alpha)}\left(1 - \frac{\Lambda_B}{d_B X_B}\right)\dot{X}_B.\end{aligned}$$

From Equations (7)–(11) we get

$$\begin{aligned}\frac{d\mathcal{F}_0}{dt} =& \left(1 - \frac{\Lambda_u}{d_u X_u}\right)(\Lambda_u - d_u X_u - \beta X_u X_v) + \frac{\nu}{\nu + d_l\alpha}((1 - \alpha)\beta X_u X_v - \nu X_l - d_l X_l) \\ &+ \frac{\nu + d_l}{\nu + d_l\alpha}(\alpha\beta X_u X_v + \nu X_l - d_i X_i) + \frac{d_i(\nu + d_l)}{r_v(\nu + d_l\alpha)}(r_v X_i - d_v X_v - \eta X_v X_B) \\ &+ \frac{d_i\eta(\nu + d_l)}{r_v\varepsilon(\nu + d_l\alpha)}\left(1 - \frac{\Lambda_B}{d_B X_B}\right)(\Lambda_B + \varepsilon X_v X_B - d_B X_B).\end{aligned}$$

Collecting terms we get

$$\begin{aligned}\frac{d\mathcal{F}_0}{dt} =& \left(1 - \frac{\Lambda_u}{d_u X_u}\right)(\Lambda_u - d_u X_u) + \beta\frac{\Lambda_u}{d_u} X_v - \frac{d_i d_v(\nu + d_l)}{r_v(\nu + d_l\alpha)} X_v \\ &+ \frac{d_i\eta(\nu + d_l)}{r_v\varepsilon(\nu + d_l\alpha)}\left(1 - \frac{\Lambda_B}{d_B X_B}\right)(\Lambda_B - d_B X_B) - \frac{d_i\eta(\nu + d_l)}{r_v(\nu + d_l\alpha)}\frac{\Lambda_B}{d_B} X_v.\end{aligned}$$

Then, we obtain

$$\begin{aligned}\frac{d\mathcal{F}_0}{dt} =& -\frac{d_u}{X_u}\left(X_u-\frac{\Lambda_u}{d_u}\right)^2+\beta\frac{\Lambda_u}{d_u}X_v-\frac{d_id_v(\nu+d_l)}{r_v(\nu+d_l\alpha)}X_v-\frac{d_Bd_i\eta(\nu+d_l)}{r_v\varepsilon(\nu+d_l\alpha)X_B}\left(X_B-\frac{\Lambda_B}{d_B}\right)^2\\&-\frac{d_i\eta(\nu+d_l)}{r_v(\nu+d_l\alpha)}\frac{\Lambda_B}{d_B}X_v\\=&-\frac{d_u}{X_u}\left(X_u-\frac{\Lambda_u}{d_u}\right)^2-\frac{d_Bd_i\eta(\nu+d_l)}{r_v\varepsilon(\nu+d_l\alpha)X_B}\left(X_B-\frac{\Lambda_B}{d_B}\right)^2\\&+\left(\beta\frac{\Lambda_u}{d_u}-\frac{d_id_v(\nu+d_l)}{r_v(\nu+d_l\alpha)}-\frac{d_i\eta(\nu+d_l)}{r_v(\nu+d_l\alpha)}\frac{\Lambda_B}{d_B}\right)X_v\\=&-\frac{d_u}{X_u}\left(X_u-\frac{\Lambda_u}{d_u}\right)^2-\frac{d_Bd_i\eta(\nu+d_l)}{r_v\varepsilon(\nu+d_l\alpha)X_B}\left(X_B-\frac{\Lambda_B}{d_B}\right)^2\\&+\frac{d_i(\nu+d_l)(d_vd_B+\eta\Lambda_B)}{r_vd_B(\nu+d_l\alpha)}(\mathcal{R}_0-1)X_v.\end{aligned}$$

Hence, $\frac{d\mathcal{F}_0}{dt}\leq 0$ is satisfied if $\mathcal{R}_0\leq 1$. Furthermore, $\frac{d\mathcal{F}_0}{dt}=0$ when $X_u=\frac{\Lambda_u}{d_u}$, $X_B=\frac{\Lambda_B}{d_B}$, $(\mathcal{R}_0-1)X_v=0$. Solutions of the system converge to the largest invariant subset [53] of $\left\{(X_u,X_l,X_i,X_v,X_B):\frac{d\mathcal{F}_0}{dt}=0\right\}=\{\mathcal{E}_0\}$. Applying LaSalle's Invariance Principle [36], we get that $\mathcal{E}_0$ is GAS. □

Appendix A.2. Proof of Theorem 2

Proof of Theorem 2. We assume $\mathcal{R}_0>1$, so the endemic equilibrium $\mathcal{E}^*=(X_u^*,X_l^*,X_i^*,X_v^*,X_B^*)$ exists and is unique. Consider a candidate Lyapunov function $\mathcal{F}^*(X_u,X_l,X_i,X_v,X_B)$:

$$\begin{aligned}\mathcal{F}^*=&X_u^*H\left(\frac{X_u}{X_u^*}\right)+\frac{\nu}{(\nu+d_l\alpha)}X_l^*H\left(\frac{X_l}{X_l^*}\right)+\frac{(\nu+d_l)}{(\nu+d_l\alpha)}X_i^*H\left(\frac{X_i}{X_i^*}\right)\\&+\frac{d_i(\nu+d_l)}{r_v(\nu+d_l\alpha)}X_v^*H\left(\frac{X_v}{X_v^*}\right)+\frac{d_i\eta(\nu+d_l)}{r_v\varepsilon(\nu+d_l\alpha)}X_B^*H\left(\frac{X_B}{X_B^*}\right).\end{aligned}$$

By Lemma 2, when $\mathcal{R}_0>1$, the endemic equilibrium E^* exists and is unique. Therefore, the Lyapunov function is well-defined.

Calculating $\frac{d\mathcal{F}^*}{dt}$, we get

$$\begin{aligned}\frac{d\mathcal{F}^*}{dt}=&\left(1-\frac{X_u^*}{X_u}\right)\dot{X}_u+\frac{\nu}{(\nu+d_l\alpha)}\left(1-\frac{X_l^*}{X_l}\right)\dot{X}_l+\frac{(\nu+d_l)}{(\nu+d_l\alpha)}\left(1-\frac{X_i^*}{X_i}\right)\dot{X}_i\\&+\frac{d_i(\nu+d_l)}{r_v(\nu+d_l\alpha)}\left(1-\frac{X_v^*}{X_v}\right)\dot{X}_v+\frac{d_i\eta(\nu+d_l)}{r_v\varepsilon(\nu+d_l\alpha)}\left(1-\frac{X_B^*}{X_B}\right)\dot{X}_B.\end{aligned}$$

From system (7)–(11) we get

$$\begin{aligned}\frac{d\mathcal{F}^*}{dt}=&\left(1-\frac{X_u^*}{X_u}\right)(\Lambda_u-d_uX_u-\beta X_uX_v)\\&+\frac{\nu}{(\nu+d_l\alpha)}\left(1-\frac{X_l^*}{X_l}\right)((1-\alpha)\beta X_uX_v-\nu X_l-d_lX_l)\end{aligned}$$

$$+\frac{(\nu+d_l)}{(\nu+d_l\alpha)}\left(1-\frac{X_i^*}{X_i}\right)(\alpha\beta X_uX_v+\nu X_l-d_iX_i)$$
$$+\frac{d_i(\nu+d_l)}{r_v(\nu+d_l\alpha)}\left(1-\frac{X_v^*}{X_v}\right)(r_vX_i-d_vX_v-\eta X_vX_B)$$
$$+\frac{d_i\eta(\nu+d_l)}{r_v\varepsilon(\nu+d_l\alpha)}\left(1-\frac{X_B^*}{X_B}\right)(\Lambda_B+\varepsilon X_vX_B-d_BX_B).$$

Collecting terms:

$$\begin{aligned}\frac{d\mathcal{F}^*}{dt}=&\left(1-\frac{X_u^*}{X_u}\right)(\Lambda_u-d_uX_u)+\beta X_u^*X_v-\frac{\nu(1-\alpha)}{(\nu+d_l\alpha)}\frac{X_l^*}{X_l}\beta X_uX_v+\frac{\nu(\nu+d_l)}{(\nu+d_l\alpha)}X_l^*\\&-\frac{\alpha(\nu+d_l)}{(\nu+d_l\alpha)}\frac{X_i^*}{X_i}\beta X_uX_v-\frac{\nu(\nu+d_l)}{(\nu+d_l\alpha)}\frac{X_i^*}{X_i}X_l+\frac{d_i(\nu+d_l)}{(\nu+d_l\alpha)}X_i^*-\frac{d_i(\nu+d_l)}{(\nu+d_l\alpha)}\frac{X_v^*}{X_v}X_i\\&-\frac{d_id_v(\nu+d_l)}{r_v(\nu+d_l\alpha)}X_v+\frac{d_i\eta(\nu+d_l)}{r_v(\nu+d_l\alpha)}X_v^*X_B+\frac{d_i\eta(\nu+d_l)}{r_v\varepsilon(\nu+d_l\alpha)}\left(1-\frac{X_B^*}{X_B}\right)(\Lambda_B-d_BX_B)\\&-\frac{d_i\eta(\nu+d_l)}{r_v(\nu+d_l\alpha)}X_vX_B^*.\end{aligned}$$

Applying the equilibrium conditions,

$$\begin{cases}\Lambda_u=d_uX_u^*+\beta X_u^*X_v^*,\\(1-\alpha)\beta X_u^*X_v^*=(\nu+d_l)X_l^*,\\\alpha\beta X_u^*X_v^*+\nu X_l^*=d_iX_i^*,\\r_vX_i^*=d_vX_v^*+\eta X_v^*X_B^*,\\\Lambda_B=-\varepsilon X_v^*X_B^*+d_BX_B^*,\end{cases}$$

we obtain

$$\begin{aligned}\frac{d\mathcal{F}^*}{dt}=&-d_u\left(\frac{(X_u-X_u^*)^2}{X_u}\right)-\frac{d_Bd_i\eta(\nu+d_l)}{r_v\varepsilon(\nu+d_l\alpha)}\frac{(X_B-X_B^*)^2}{X_B}+\left(1-\frac{X_u^*}{X_u}\right)\beta X_u^*X_v^*+\beta X_u^*X_v\\&-\frac{\nu(1-\alpha)}{(\nu+d_l\alpha)}\frac{X_l^*}{X_l}\beta X_uX_v+\frac{\nu(\nu+d_l)}{(\nu+d_l\alpha)}X_l^*-\frac{\alpha(\nu+d_l)}{(\nu+d_l\alpha)}\frac{X_i^*}{X_i}\beta X_uX_v-\frac{\nu(\nu+d_l)}{(\nu+d_l\alpha)}\frac{X_i^*}{X_i}X_l\\&+\frac{d_i(\nu+d_l)}{(\nu+d_l\alpha)}X_i^*-\frac{d_i(\nu+d_l)}{(\nu+d_l\alpha)}\frac{X_v^*}{X_v}X_i-\frac{d_id_v(\nu+d_l)}{r_v(\nu+d_l\alpha)}X_v+\frac{d_id_v(\nu+d_l)}{r_v(\nu+d_l\alpha)}X_v^*\\&+\frac{d_i\eta(\nu+d_l)}{r_v(\nu+d_l\alpha)}X_v^*X_B-\frac{d_i\eta(\nu+d_l)}{r_v(\nu+d_l\alpha)}\left(1-\frac{X_B^*}{X_B}\right)X_v^*X_B^*-\frac{d_i\eta(\nu+d_l)}{r_v(\nu+d_l\alpha)}X_vX_B^*.\end{aligned}$$

Finally, after simplifications using the equilibrium conditions, we obtain

$$\begin{aligned}\frac{d\mathcal{F}^*}{dt}=&-d_u\frac{(X_u-X_u^*)^2}{X_u}-\frac{d_Bd_i\eta(\nu+d_l)}{r_v\varepsilon(\nu+d_l\alpha)}\frac{(X_B-X_B^*)^2}{X_B}\\&+\frac{(\nu+d_l)}{(\nu+d_l\alpha)}\alpha\beta X_u^*X_v^*\left(3-\frac{X_u^*}{X_u}-\frac{X_i^*X_uX_v}{X_iX_u^*X_v^*}-\frac{X_v^*X_i}{X_vX_i^*}\right)\\&+\frac{\nu}{(\nu+d_l\alpha)}(1-\alpha)\beta X_u^*X_v^*\left(4-\frac{X_u^*}{X_u}-\frac{X_l^*X_uX_v}{X_lX_u^*X_v^*}-\frac{X_i^*X_l}{X_iX_l^*}-\frac{X_v^*X_i}{X_vX_i^*}\right).\end{aligned}$$

We obtain that $\frac{d\mathcal{F}^*}{dt}\leq 0$. Moreover, $\frac{d\mathcal{F}^*}{dt}=0$ if $X_u=X_u^*$, $X_l=X_l^*$, $X_i=X_i^*$, $X_v=X_v^*$, $X_B=X_B^*$. Solutions of the model converge to $\mathcal{E}^*$. Consequently, LaSalle's Invariance Principle [36] reveals that $\mathcal{E}^*$ is GAS. □

Appendix B. Proof of Theorems 3 and 4

Appendix B.1. Proof of Theorem 3

Proof of Theorem 3. Define the candidate Lyapunov function $\mathcal{F}_0^d(X_u, X_l, X_i, X_v, X_B)$ as

$$\begin{aligned}\mathcal{F}_0^d &= K\frac{\Lambda_u}{d_u}H\left(\frac{d_uX_u}{\Lambda_u}\right) + \nu F_3X_l + (\nu+d_l)X_i + \frac{d_i(\nu+d_l)}{r_vF_4}X_v + \frac{d_i\eta(\nu+d_l)}{r_v\varepsilon F_4}\frac{\Lambda_B}{d_B}H\left(\frac{d_BX_B}{\Lambda_B}\right)\\ &+ \nu\beta(1-\alpha)F_3\int_0^{\omega_1}\Pi_1(\tau)\int_{t-\tau}^{t}X_u(\theta)X_v(\theta)\,d\theta d\tau\\ &+ \alpha\beta(\nu+d_l)\int_0^{\omega_2}\Pi_2(\tau)\int_{t-\tau}^{t}X_u(\theta)X_v(\theta)\,d\theta d\tau\\ &+ \nu(\nu+d_l)\int_0^{\omega_3}\Pi_3(\tau)\int_{t-\tau}^{t}X_l(\theta)\,d\theta d\tau + \frac{d_i(\nu+d_l)}{F_4}\int_0^{\omega_4}\Pi_4(\tau)\int_{t-\tau}^{t}X_i(\theta)\,d\theta d\tau.\end{aligned}$$

Obviously, $\mathcal{F}_0^d(X_u, X_l, X_i, X_v, X_B) > 0$ for any $X_u, X_l, X_i, X_v, X_B > 0$, and $\mathcal{F}_0^d\left(\frac{\Lambda_u}{d_u}, 0, 0, 0, \frac{\Lambda_B}{d_B}\right) = 0$.

Let us calculate $\frac{d\mathcal{F}_0^d}{dt}$ along the solutions of model (1)–(5):

$$\begin{aligned}\frac{d\mathcal{F}_0^d}{dt} &= K\left(1-\frac{\Lambda_u}{d_uX_u}\right)\dot{X}_u + \nu F_3\dot{X}_l + (\nu+d_l)\dot{X}_i + \frac{d_i(\nu+d_l)}{r_vF_4}\dot{X}_v\\ &+ \frac{d_i\eta(\nu+d_l)}{r_v\varepsilon F_4}\left(1-\frac{\Lambda_B}{d_BX_B}\right)\dot{X}_B + \nu\beta(1-\alpha)F_3\int_0^{\omega_1}\Pi_1(\tau)(X_uX_v - X_u(t-\tau)X_v(t-\tau))d\tau\\ &+ \alpha\beta(\nu+d_l)\int_0^{\omega_2}\Pi_2(\tau)(X_uX_v - X_u(t-\tau)X_v(t-\tau))d\tau\\ &+ \nu(\nu+d_l)\int_0^{\omega_3}\Pi_3(\tau)(X_l - X_l(t-\tau))d\tau + \frac{d_i(\nu+d_l)}{F_4}\int_0^{\omega_4}\Pi_4(\tau)(X_i - X_i(t-\tau))d\tau.\end{aligned}$$

Using Equations (1)–(5), we obtain

$$\begin{aligned}\frac{d\mathcal{F}_0^d}{dt} &= K\left(1-\frac{\Lambda_u}{d_uX_u}\right)(\Lambda_u - d_uX_u - \beta X_uX_v)\\ &+ \nu F_3\left((1-\alpha)\beta\int_0^{\omega_1}\Pi_1(\tau)X_u(t-\tau)X_v(t-\tau)\,d\tau - (\nu+d_l)X_l\right)\\ &+ (\nu+d_l)\left(\alpha\beta\int_0^{\omega_2}\Pi_2(\tau)X_u(t-\tau)X_v(t-\tau)\,d\tau + \nu\int_0^{\omega_3}\Pi_3(\tau)X_l(t-\tau)\,d\tau - d_iX_i\right)\\ &+ \frac{d_i(\nu+d_l)}{r_vF_4}\left(r_v\int_0^{\omega_4}\Pi_4(\tau)X_i(t-\tau)\,d\tau - d_vX_v - \eta X_vX_B\right)\\ &+ \frac{d_i\eta(\nu+d_l)}{r_v\varepsilon F_4}\left(1-\frac{\Lambda_B}{d_BX_B}\right)(\Lambda_B + \varepsilon X_vX_B - d_BX_B)\\ &+ \nu\beta(1-\alpha)F_3\int_0^{\omega_1}\Pi_1(\tau)(X_uX_v - X_u(t-\tau)X_v(t-\tau))d\tau\\ &+ \alpha\beta(\nu+d_l)\int_0^{\omega_2}\Pi_2(\tau)(X_uX_v - X_u(t-\tau)X_v(t-\tau))d\tau\\ &+ \nu(\nu+d_l)\int_0^{\omega_3}\Pi_3(\tau)(X_l - X_l(t-\tau))d\tau + \frac{d_i(\nu+d_l)}{F_4}\int_0^{\omega_4}\Pi_4(\tau)(X_i - X_i(t-\tau))d\tau.\end{aligned}$$

Collecting terms, we obtain

$$\begin{aligned}\frac{d\mathcal{F}_0^d}{dt} &= -K\frac{d_u}{X_u}\left(X_u - \frac{\Lambda_u}{d_u}\right)^2 - \frac{d_i\eta(\nu+d_l)}{r_v\varepsilon F_4}\frac{d_B}{X_B}\left(X_B - \frac{\Lambda_B}{d_B}\right)^2 + \left(K\beta\frac{\Lambda_u}{d_u} - 1\right)X_v\\ &= -K\frac{d_u}{X_u}\left(X_u - \frac{\Lambda_u}{d_u}\right)^2 - \frac{d_i\eta(\nu+d_l)}{r_v\varepsilon F_4}\frac{d_B}{X_B}\left(X_B - \frac{\Lambda_B}{d_B}\right)^2\\ &+ \frac{d_i(\nu+d_l)(d_vd_B + \eta\Lambda_B)}{r_vd_BF_4}(\mathcal{R}_0^d - 1)X_v.\end{aligned}$$

When $\mathcal{R}_0^d \leq 1$, then $\frac{d\mathcal{F}_0^d}{dt} \leq 0$. Furthermore, $\frac{d\mathcal{F}_0^d}{dt} = 0$ when $X_u = \frac{\Lambda_u}{d_u}$, $X_B = \frac{\Lambda_B}{d_B}$, and $(\mathcal{R}_0^d - 1)X_v = 0$. Solutions of the model (1)–(5) converge to the largest invariant subset of $\left\{(X_u, X_l, X_i, X_v, X_B) : \frac{d\mathcal{F}_0^d}{dt} = 0\right\} = \{\mathcal{E}_0^d\}$. Applying the Lyapunov-LaSalle asymptotic stability theorem [32], we get that $\mathcal{E}_0^d$ is GAS. □

Appendix B.2. Proof of Theorem 4

Proof of Theorem 4. Construct $\mathcal{F}_d^*(X_u, X_l, X_i, X_v, X_B)$:

$$\begin{aligned}
\mathcal{F}_d^* &= KX_u^* H\left(\frac{X_u}{X_u^*}\right) + \nu F_3 X_l^* H\left(\frac{X_l}{X_l^*}\right) + (\nu + d_l)X_i^* H\left(\frac{X_i}{X_i^*}\right) + \frac{d_i(\nu + d_l)}{r_v F_4} X_v^* H\left(\frac{X_v}{X_v^*}\right) \\
&+ \frac{d_i \eta(\nu + d_l)}{r_v \varepsilon F_4} X_B^* H\left(\frac{X_B}{X_B^*}\right) + \nu\beta(1-\alpha)F_3 X_u^* X_v^* \int_0^{\omega_1} \Pi_1(\tau) \int_{t-\tau}^{t} H\left(\frac{X_u(\theta)X_v(\theta)}{X_u^* X_v^*}\right) d\theta d\tau \\
&+ \alpha\beta(\nu + d_l)X_u^* X_v^* \int_0^{\omega_2} \Pi_2(\tau) \int_{t-\tau}^{t} H\left(\frac{X_u(\theta)X_v(\theta)}{X_u^* X_v^*}\right) d\theta d\tau \\
&+ \nu(\nu + d_l)X_l^* \int_0^{\omega_3} \Pi_3(\tau) \int_{t-\tau}^{t} H\left(\frac{X_l(\theta)}{X_l^*}\right) d\theta d\tau \\
&+ \frac{d_i(\nu + d_l)}{F_4} X_i^* \int_0^{\omega_4} \Pi_4(\tau) \int_{t-\tau}^{t} H\left(\frac{X_i(\theta)}{X_i^*}\right) d\theta d\tau.
\end{aligned}$$

By Lemma 4, when $\mathcal{R}_0^d > 1$, the endemic equilibrium $\mathcal{E}_d^*$ exists and is unique. Therefore, the Lyapunov function is well-defined.

Take the derivative of $\mathcal{F}_d^*$ along the solution of model (1)–(5):

$$\begin{aligned}
\frac{d\mathcal{F}_d^*}{dt} &= K\left(1 - \frac{X_u^*}{X_u}\right)(\Lambda_u - d_u X_u - \beta X_u X_v) \\
&+ \nu F_3 \left(1 - \frac{X_l^*}{X_l}\right)\left((1-\alpha)\beta \int_0^{\omega_1} \Pi_1(\tau) X_u(t-\tau) X_v(t-\tau) d\tau - (\nu + d_l)X_l\right) \\
&+ (\nu + d_l)\left(1 - \frac{X_i^*}{X_i}\right)\left(\alpha\beta \int_0^{\omega_2} \Pi_2(\tau) X_u(t-\tau) X_v(t-\tau) d\tau + \nu \int_0^{\omega_3} \Pi_3(\tau) X_l(t-\tau) d\tau - d_i X_i\right) \\
&+ \frac{d_i(\nu + d_l)}{r_v F_4}\left(1 - \frac{X_v^*}{X_v}\right)\left(r_v \int_0^{\omega_4} \Pi_4(\tau) X_i(t-\tau) d\tau - d_v X_v - \eta X_v X_B\right) \\
&+ \frac{d_i \eta(\nu + d_l)}{r_v \varepsilon F_4}\left(1 - \frac{X_B^*}{X_B}\right)(\Lambda_B + \varepsilon X_v X_B - d_B X_B) \\
&+ \nu\beta(1-\alpha)F_3 X_u^* X_v^* \int_0^{\omega_1} \Pi_1(\tau)\left[\frac{X_u X_v}{X_u^* X_v^*} - \frac{X_u(t-\tau)X_v(t-\tau)}{X_u^* X_v^*} + \ln\left(\frac{X_u(t-\tau)X_v(t-\tau)}{X_u X_v}\right)\right] d\tau \\
&+ \alpha\beta(\nu + d_l)X_u^* X_v^* \int_0^{\omega_2} \Pi_2(\tau)\left[\frac{X_u X_v}{X_u^* X_v^*} - \frac{X_u(t-\tau)X_v(t-\tau)}{X_u^* X_v^*} + \ln\left(\frac{X_u(t-\tau)X_v(t-\tau)}{X_u X_v}\right)\right] d\tau \\
&+ \nu(\nu + d_l)X_l^* \int_0^{\omega_3} \Pi_3(\tau)\left[\frac{X_l}{X_l^*} - \frac{X_l(t-\tau)}{X_l^*} + \ln\left(\frac{X_l(t-\tau)}{X_l}\right)\right] d\tau \\
&+ \frac{d_i(\nu + d_l)}{F_4} X_i^* \int_0^{\omega_4} \Pi_4(\tau)\left[\frac{X_i}{X_i^*} - \frac{X_i(t-\tau)}{X_i^*} + \ln\left(\frac{X_i(t-\tau)}{X_i}\right)\right] d\tau.
\end{aligned}$$

Summing the terms and using the following equilibrium conditions,

$$(1-\alpha)F_1\beta X_u^* X_v^* = (\nu + d_l)X_l^*, \quad \alpha F_2 \beta X_u^* X_v^* + \nu F_3 X_l^* = d_i X_i^*, r_v F_4 X_i^* = d_v X_v^* + \eta X_v^* X_B^*,$$
$$\Lambda_B = d_B X_B^* - \varepsilon X_v^* X_B^*,$$

we obtain

$$\begin{aligned}\frac{d\mathcal{F}_d^*}{dt} &= -K\frac{d_u}{X_u}(X_u - X_u^*)^2 - \frac{d_i\eta(\nu+d_l)}{r_v\varepsilon F_4}\frac{\Lambda_B}{X_B X_B^*}(X_B - X_B^*)^2 - KH\left(\frac{X_u^*}{X_u}\right)\beta X_u^* X_v^* \\ &\quad - \nu\beta(1-\alpha)F_3 X_u^* X_v^* \int_0^{\omega_1}\Pi_1(\tau)H\left(\frac{X_u(t-\tau)X_v(t-\tau)X_l^*}{X_u^* X_v^* X_l}\right)d\tau \\ &\quad - \alpha\beta(\nu+d_l)X_u^* X_v^* \int_0^{\omega_2}\Pi_2(\tau)H\left(\frac{X_u(t-\tau)X_v(t-\tau)X_i^*}{X_u^* X_v^* X_i}\right)d\tau \\ &\quad - \nu(\nu+d_l)X_l^* \int_0^{\omega_3}\Pi_3(\tau)H\left(\frac{X_l(t-\tau)X_i^*}{X_l^* X_i}\right)d\tau - \frac{d_i(\nu+d_l)}{F_4}X_i^* \int_0^{\omega_4}\Pi_4(\tau)H\left(\frac{X_i(t-\tau)X_v^*}{X_i^* X_v}\right)d\tau.\end{aligned}$$

Obviously, $\frac{d\mathcal{F}_d^*}{dt} \leq 0$ for any $X_u, X_l, X_i, X_v, X_B > 0$. Moreover, $\frac{d\mathcal{F}_d^*}{dt} = 0$ if $X_u = X_u^*$, $X_l = X_l^*$, $X_i = X_i^*$, $X_v = X_v^*$, and $X_B = X_B^*$. Solutions of the model converge to the largest invariant subset of $\left\{(X_u, X_l, X_i, X_v, X_B) : \frac{d\mathcal{F}_d^*}{dt} = 0\right\}$ where $X_u = X_u^*$, $X_l = X_l^*$, $X_i = X_i^*$, $X_v = X_v^*$, and $X_B = X_B^*$. Thus, by the Lyapunov-LaSalle asymptotic stability theorem, $\mathcal{E}_d^*$ is GAS. □

References

1. UNAIDS. *Global HIV & AIDS Statistics—Fact Sheet*; UNAIDS: Geneva, Switzerland , 2025.
2. Chun, T.W.; Stuyver, L.; Mizell, S.B.; Ehler, L.A.; Mican, J.A.M.; Baseler, M.; Lloyd, A.L.; Nowak, M.A.; Fauci, A.S. Presence of an inducible HIV-1 latent reservoir during highly active antiretroviral therapy. *Proc. Natl. Acad. Sci. USA* **1997**, *94*, 13193–13197. [CrossRef]
3. Finzi, D.; Hermankova, M.; Pierson, T.; Carruth, L.M.; Buck, C.; Chaisson, R.E.; Quinn, T.C.; Chadwick, K.; Margolick, J.; Brookmeyer, R.; et al. Identification of a reservoir for HIV-1 in patients on highly active antiretroviral therapy. *Science* **1997**, *278*, 1295–1300. [CrossRef]
4. Chun, T.; Fauci, A. Latent reservoirs of HIV: Obstacles to the eradication of virus. *Proc. Natl. Acad. Sci. USA* **1999**, *96*, 10958–10961. [CrossRef] [PubMed]
5. Siliciano, J.M.; Siliciano, R.F. The Latent Reservoir for HIV-1 in Resting CD4$^+$ T Cells: A Barrier to Cure. *Curr. Opin. HIV AIDS* **2006**, *1*, 121–128. [CrossRef]
6. Herz, A.; Bonhoeffer, S.; Anderson, R.; May, R.; Nowak, M. Viral dynamics in vivo: Limitations on estimates of intracellular delay and virus decay. *Proc. Natl. Acad. Sci. USA* **1996**, *93*, 7247—7251. [CrossRef]
7. Perelson, A.S.; Neumann, A.U.; Markowitz, M.; Leonard, J.M.; Ho, D.D. HIV-1 dynamics in vivo: Virion clearance rate, infected cell life-span, and viral generation time. *Science* **1996**, *271*, 1582–1586. [CrossRef]
8. Hammer, S.M.; Squires, K.E.; Hughes, M.D.; Grimes, J.M.; Demeter, L.M.; Currier, J.S.; Fischl, M.A.; Phair, J.P.; Pedneault, L.; Nguyen, B.-Y.; et al. A controlled trial of two nucleoside analogues plus indinavir in persons with human immunodeficiency virus infection and CD4 cell counts of 200 per cubic millimeter or less. *N. Engl. J. Med.* **1997**, *337*, 725–733. [CrossRef]
9. Gulick, R.M.; Mellors, J.W.; Havlir, D.; Eron, J.J.; Gonzalez, C.; McMahon, D.; Richman, D.D.; Valentine, F.T.; Jonas, L.; Meibohm, A.; et al. Treatment with indinavir, zidovudine, and lamivudine in adults with human immunodeficiency virus infection and prior antiretroviral therapy. *N. Engl. J. Med.* **1997**, *337*, 734–739. [CrossRef]
10. Paterson, D.; Swindells, S.; Mohr, J.; Brender, M.; Vergis, E.N.; Squier, C.; Wagener, M.M.; Singh, N. Adherence to protease inhibitor therapy and outcomes in patients with HIV infection. *Ann. Intern. Med.* **2000**, *133*, 21–30. [CrossRef]
11. Hightower, K.; Wang, R.; Deanda, F.; Jones, G.S.; Jobse, B.; Weaver, K.; Shen, Y.; Tomberlin, G.H.; Carter, H.L., III; Broderick, T.; et al. Dolutegravir (S/GSK1349572) exhibits significantly slower dissociation than raltegravir and elvitegravir from wild-type and integrase inhibitor-resistant HIV-1 integrase-DNA complexes. *Antimicrob. Agents Chemother.* **2011**, *55*, 4552–4559. [CrossRef]
12. Nowak, M.A.; Bonhoeffer, S.; Hill, A.M.; Boehme, R.; Thomas, H.C.; McDade, H. Viral dynamics in hepatitis B virus infection. *Proc. Natl. Acad. Sci. USA* **1996**, *93*, 4398–4402. [CrossRef]
13. Fister, K.R.; Lenhart, S.; McNally, J.S. Optimizing chemotherapy in an HIV model. *Electron. J. Differ. Equ.* **1998**, *32*, 1–12.
14. Culshaw, R.V.; Ruan, S. A delay-differential equation model of HIV infection of CD4$^+$ T-cells. *Math. Biosci.* **2000**, *165*, 27–39. [CrossRef]
15. Blunu, C.P.; Mushayabasa, S.; Kojouharov, H.; Tchuenche, J.M. Mathematical Analysis of an HIV/AIDS Model: Impact of Educational Programs and Abstinence in Sub-Saharan Africa. *J. Math. Model. Algor.* **2011**, *10*, 31–55. [CrossRef]
16. Conway, J.M.; Perelson, A.S. Post-treatment control of HIV infection. *Proc. Natl. Acad. Sci. USA* **2015**, *112*, 5467–5472. [CrossRef] [PubMed]

17. Kruize, Z.; Kootstra, N.A. The Role of Macrophages in HIV-1 Persistence and Pathogenesis. *Front. Microbiol.* **2019**, *10*, 2828. [CrossRef] [PubMed]
18. Prakash, S.; Umrao, A.; Srivastava, P. Bifurcation and stability analysis of within host HIV dynamics with multiple infections and intracellular delay. *Chaos* **2025**, *35*, 013128. [CrossRef]
19. Lv, L.; Yang, J.; Hu, Z.; Fan, D. Dynamics Analysis of a Delayed HIV Model with Latent Reservoir and Both Viral and Cellular Infections. *Math. Methods Appl. Sci.* **2025**, *48*, 6063–6080. [CrossRef]
20. Alharbi, M.H. Global investigation for an "SIS" model for COVID-19 epidemic with asymptomatic infection. *Math. Biosci. Eng.* **2023**, *20*, 5298–5315. [CrossRef] [PubMed]
21. Nath, B.J.; Dehingia, K.; Sadri, K.; Sarmah, H.K.; Hosseini, K.; Park, C. Optimal control of combined antiretroviral therapies in an HIV infection model with cure rate and fusion effect. *Int. J. Biomath.* **2023**, *16*, 2250062. [CrossRef]
22. Murase, A.; Sasaki, T.; Kajiwara, T. Stability analysis of pathogen-immune interaction dynamics. *J. Math. Biol.* **2005**, *51*, 247–267. [CrossRef]
23. Ganusov, V.V.; Neher, R.A.; Perelson, A.S. Mathematical modeling of escape of HIV from cytotoxic T lymphocyte responses. *J. Stat. Mech.* **2013**, *2013*, P01010. [CrossRef]
24. Nelson, P.W.; Perelson, A.S. Mathematical analysis of delay differential equation models of HIV-1 infection. *Math. Biosci.* **2002**, *179*, 73–94. [CrossRef] [PubMed]
25. Rong, L.; Feng, Z.; Perelson, A.S. Mathematical analysis of age-structured HIV-1 dynamics with combination antiretroviral therapy. *SIAM* **2007**, *67*, 26. [CrossRef]
26. Li, Y.; Zhang, L.; Zhang, J.; Liu, S.; Peng, Z. Dynamical modeling and data analysis of HIV infection with infection-age, CTLs immune response and delayed antibody immune response. *J. Math. Biol.* **2025**, *91*, 57. [CrossRef] [PubMed]
27. Alalhareth, F.K.; Alghamdi, F.K.; Alharbi, M.H.; El Hajji, M. Global Dynamics and Optimal Control of a Dual-Target HIV Model with Latent Reservoirs. *Mathematics* **2025**, *13*, 3868. [CrossRef]
28. Almuashi, H.H.; El Hajji, M. Global Dynamics of a Dual-Target HIV Model with Time Delays and Treatment Implications. *Mathematics* **2026**, *14*, 6. [CrossRef]
29. El Hajji, M.; Alnjrani, R.M. Periodic Behaviour of HIV Dynamics with Three Infection Routes. *Mathematics* **2024**, *12*, 123. [CrossRef]
30. El Hajji, M.; Alnjrani, R.M. Periodic Trajectories for HIV Dynamics in a Seasonal Environment with a General Incidence Rate. *Int. J. Anal. Appl.* **2023**, *21*, 96. [CrossRef]
31. Alharbi, M.H. HIV dynamics in a periodic environment with general transmission rates. *AIMS Math.* **2024**, *9*, 31393–31413. [CrossRef]
32. Korobeinikov, A. Global properties of basic virus dynamics models. *Bull. Math. Biol.* **2004**, *66*, 879–883. [CrossRef]
33. Diekmann, O.; Heesterbeek, J. On the definition and the computation of the basic reproduction ratio $\mathcal{R}_0$ in models for infectious diseases in heterogeneous populations. *J. Math. Bio.* **1990**, *28*, 365–382. [CrossRef]
34. Van den Driessche, P.; Watmough, J. Reproduction Numbers and Sub-Threshold Endemic Equilibria for Compartmental Models of Disease Transmission. *Math. Biosci.* **2002**, *180*, 29–48. [CrossRef] [PubMed]
35. Almuallem, N.A.; El Hajji, M. Global Dynamics of a Multi-Population Water Pollutant Model with Distributed Delays. *Mathematics* **2026**, *14*, 20. [CrossRef]
36. Khalil, H. *Nonlinear Systems*, 2nd ed.: Prentice Hall: Hoboken, NJ, USA, 1996.
37. El Hajji, M.; Al-Faidi, Y.A.; Alharbi, M.H. Modeling dual-colony Nosema transmission in honeybees: The role of distributed delays and antiviral treatment. *AIMS Math.* **2026**, *11*, 2645–2681. [CrossRef]
38. Al-arydah, M. Assessing vaccine efficacy for infectious diseases with variable immunity using a mathematical model. *Sci. Rep.* **2024**, *14*, 18572. [CrossRef]
39. Perelson, A.S.; Kirschner, D.E.; Boer, R.D. Dynamics of HIV-1 infection of $CD4^+$ T cells. *Math. Biosci.* **1993**, *114*, 81–125. [CrossRef]
40. Lin, J.; Xu, R.; Tian, X. Threshold dynamics of an HIV-1 virus model with both virus-to-cell and cell-to-cell transmissions, intracellular delay, and humoral immunity. *Appl. Math. Comput.* **2017**, *315*, 516–530. [CrossRef]
41. Hadjiandreou, M.; Conejeros, R.; Vassiliadis, V.S. Towards a long-term model construction for the dynamic simulation of HIV-1 infection. *Math. Biosci. Eng.* **2007**, *4*, 489–504. [CrossRef]
42. Hernandez-Vargas, E.A.; Middleton, R.H. Modeling the three stages in HIV infection. *J. Theor. Biol.* **2013**, *320*, 33–40. [CrossRef]
43. Szomolay, B.; Lungu, E.M. A mathematical model for the treatment of AIDS-related Kaposi's sarcoma. *J. Biol. Syst.* **2014**, *22*, 495–522. [CrossRef]
44. Sahani, S.K.; Yashi. Effects of eclipse phase and delay on the dynamics of HIV-1 infection. *J. Biol. Syst.* **2018**, *26*, 421–454. [CrossRef]
45. Pankavich, S. The effects of latent infection on the dynamics of HIV-1. *Differ. Equ. Dyn. Syst.* **2016**, *24*, 281–303. [CrossRef]
46. Elaiw, A.M.; Alhmadi, A.S.; Hobiny, A.D. Dynamics and stability of a within-host HIV-HBV co-infection model with time delays. *Front. Appl. Math. Stat.* **2025**, *11*, 1633039. [CrossRef]

47. Elaiw, A.M.; Alhmadi, A.S.; Hobiny, A.D. Analysis of HIV and HBV co-dynamics in vivo. *J. Math. Comput. Sci.* **2026**, *40*, 240–272. [CrossRef]
48. Chitnis, N.; Hyman, J.M.; Cushing, J.M. Determining Important Parameters in the Spread of Malaria Through the Sensitivity Analysis of a Mathematical Model. *Bull. Math. Biol.* **2008**, *70*, 1272–1296. [CrossRef] [PubMed]
49. Marino, S.; Hogue, I.B.; Ray, C.J.; Kirschner, D.E. A Methodology for Performing Global Uncertainty and Sensitivity Analysis in Systems Biology. *J. Theor. Biol.* **2008**, *254*, 178–196. [CrossRef] [PubMed]
50. Deeks, S.; Lewin, S.; Havlir, D. The end of AIDS: HIV infection as a chronic disease. *Lancet* **2014**, *382*, 1525–1533. [CrossRef]
51. Zhuang, L.; Ma, Y.; Fang, G.; Xu, A. Modeling two-scale degradation with heterogeneity: A unified random-effects inverse Gaussian framework. In *IISE Transactions*; Taylor & Francis: Oxfordshire, UK, 2026; pp. 1–16. [CrossRef]
52. Wang, Y.; Li, J.; Zhou, Q.; Wang, W. A unified framework for complex survival data: Accounting for clustering, cure fractions, and competing risks. *BMC Med. Res. Methodol.* **2026**, *26*, 105. [CrossRef]
53. Hale, J.K.; Verduyn Lunel, S.M. *Introduction to Functional Differential Equations*; Springer: New York, NY, YSA, 1993. [CrossRef]